Accepted Manuscript

Volcanic glass geochemistry of pyroclastic deposits for the last 50ka in the Aeolian Islands: A proximal database for distal tephrochronology

Paul G Albert, Emma L Tomlinson, Victoria C Smith, Federico Di Traglia, Marco Pistolesi, Anna Morris, Paola Donato, Rosanna De Rosa, Roberto Sulpizio, Jörg Keller, Mauro Rosi, Martin Menzies

Please cite this article as: Paul G Albert, Emma L Tomlinson, Victoria C Smith, Federico Di Traglia, Marco Pistolesi, Anna Morris, Paola Donato, Rosanna De Rosa, Roberto Sulpizio, Jörg Keller, Mauro Rosi, Martin Menzies , Volcanic glass geochemistry of pyroclastic deposits for the last 50ka in the Aeolian Islands: A proximal database for distal tephrochronology. The address for the corresponding author was captured as affiliation for all authors. Please check if appropriate. Volgeo(2017), doi: 10.1016/j.jvolgeores.2017.02.008

Volcanic glass geochemistry of pyroclastic deposits for the last 50 ka in the Aeolian Islands: a proximal database for distal tephrochronology

Paul G Albert[a,b]*, Emma L Tomlinson[c], Victoria C Smith[a], Federico Di Traglia[d], Marco Pistolesi[d], Anna Morris[b], Paola Donato[e], Rosanna De Rosa[e], Roberto Sulpizio[f], Jörg Keller[g], Mauro Rosi[h], Martin Menzies[b]

[a] *Research Laboratory for Archaeology and the History of Art, University of Oxford, Dyson Perrins Building, South Parks Road, Oxford, OX1 3QY, UK*

[b] *Department of Earth Sciences, Royal Holloway University of London, Egham, TW20 0EX, UK*

[c] *Department of Geology, Trinity College Dublin, Dublin 2, Ireland*

[d] *Dipartimento di Scienze della Terra, Università di Firenze, Via La Pira 4, 50121 Florence, Italy*

[e] *DiBEST Universita della Calabria, Italy*

[f] *Dipartmento di Scienze della Terra e Geoambientali, Unitversitá di Bari, via Orabona 4, 70125 Bari, Italy*

[g] *Institute of Geosciences, Mineralogy and Geochemistry, Albert-Ludwigs-University Freiburg, Albertstrasse 23b, 79104 Freiburg, Germany*

[h] *Departimento Scienza della Terra, Universita di Pisa, Via S. Maria 53-56126, Pisa, Italy*

* Corresponding author

Abstract

Volcanic ash (< 2 mm) erupted from the Aeolian Islands is reported distally as layers in sedimentary archives from across the central Mediterranean region. Here we present volcanic glass geochemistry of proximal tephra deposits from explosive eruptions on the islands of Vulcano, Lipari, Salina and Stromboli spanning approximately the last 50 ka using grain-specific EMPA and LA-ICP-MS. This comprehensive database of volcanic glass compositions (>1000 analyses) provides a basis for proximal-distal and distal-distal tephra correlations. Tephra deposits from the different Aeolian Islands are geochemically diverse; with some individual eruptions showing diagnostic geochemical heterogeneity recognised both stratigraphically and/or spatially. Major element glass analyses reveal that Vulcano (0-21ka) and Stromboli (4-13ka) have erupted potassic (shoshonitic and K-series) tephra with broadly overlapping compositions, but data presented here demonstrates that their eruptive products can be distinguished using either TiO_2 contents or their HFSE/Th ratios. Whilst individual volcanic sources often produce successive tephra deposits with near identical major and minor element compositions through time (i.e., Lipari, Vulcano), trace element glass data can help to decipher successive eruptions. Changes in LREE and Th concentrations of volcanic glasses erupted spanning approximately the last 50 ka greatly enhance the potential to discriminate successive eruptive units on Lipari. The new proximal glass database has been used to verify new (Ionian Sea; core M25/4-12) and existing distal occurrences of Aeolian Island derived tephra enabling the reassessments of past ash dispersals. Finally, proximal and distal data have been used to establish an integrated proximal-distal eruptive event stratigraphy for the Aeolian Islands.

1. Introduction

Explosive volcanism in the Aeolian Islands is responsible for the distal dispersal of tephra (volcanic ash, < 2mm). Distal occurrences of Aeolian Island derived tephra are reported within marine archives from across the central Mediterranean, including the Tyrrhenian (Paterne et al., 1986; 1988; Di Roberto et al., 2008; Albert et al. 2012), Adriatic (Siani et al., 2004; Matthews et al., 2015) and Ionian (Clift and Blusztajn, 1999; Caron et al., 2012; Insinga et al., 2014) Seas. Furthermore, Aeolian Island tephra are also recorded in terrestrial sequences from Sicily (Morche, 1988; Narcisi, 2002). These tephra layers preserved in distal sedimentary archives can provide invaluable stratigraphic markers (Tephrostratigraphy) which are suitable for precisely synchronising disparate paleoclimate records, and where the age of the eruption is known they also provide important chronostratigraphic markers (Tephrochronology) which can aid in constraining age-depth models. The increasing application of cryptotephra investigations into distal sedimentary records of the Central Mediterranean (e.g., Bourne et al., 2010; 2015; Matthews et al., 2015) also mean that there is further potential to extend the utilisation of Aeolian Islands tephra for the synchronisation and dating of paleoclimate archives. The tephrostratigraphy of these distal records offers enormous potential to help constrain the magnitude and frequency of explosive eruptions from active volcanoes, which is essential for future hazard assessments.

However, the promise of distal tephra layers for both dating and synchronising sedimentary archives relies heavily upon the detailed characterisation of their glass compositions from proximal eruptive sequences (e.g., Smith et al., 2011; Tomlinson et al., 2012a; Tomlinson et al., 2015). Detailed characterisation of proximal volcanic glasses using grain-specific multi-elemental data following micro-analytical techniques is crucial for establishing precise tephra correlations owing to the fact that; (1) whole-rock analysis of proximal tephra, incorporate phenocrysts and therefore these compositions are not directly comparable to the matrix glass found distally, which can lead to erroneous correlations (e.g., Tomlinson et al., 2012b); (2) many volcanic systems produced repeated glass chemistries (e.g., Davies et al., 2004;

Smith et al., 2011; Tomlinson et al., 2012a) and it is only through the identification of subtle diagnostic variations in trace element concentrations, which are more sensitive to fractionation processes, that it is possible to distinguish successive tephra units (Allan et al., 2008; Albert et al., 2015); (3) where successive tephra units share overlapping compositions it is often the geochemical variability observed within the products of an individual eruptions that enable their distinction from other tephra erupted from the same volcanic centre (e.g., Tomlinson et al., 2014).

The purpose of this investigation is to: (1) define the major, minor and trace element glass geochemistries of proximal deposits of some of the largest explosive eruptions recorded on the Aeolian Islands spanning approximately the last 50 ka; (2) assess the chemical variability of the glass compositions produced, both temporally and spatially; (3) identify diagnostic features useful in assigning provenance solutions to unknown distal tephra thought to derived from the Aeolian Islands; (4) use this geochemical information to help assess proximal-distal tephra correlations and established an integrated tephrostratigraphy for the islands.

2.   Geological background

The Aeolian Islands (Italy) are located in the southern Tyrrhenian Sea, situated between the Marsili oceanic basin and the Calabrian arc. The seven volcanic islands of the archipelago (Alicudi, Filicudi, Salina, Lipari, Vulcano, Panarea and Stromboli (Fig. 1)) are the emerged portion of a half-ring shaped volcanic complex that also includes seven seamounts. Magmatism in the region stared at around 1.3 Ma (Beccaluva et al., 1985). The geodynamic setting responsible for volcanic activity of the Aeolian Island is still debated. On the basis of geochemical features and a NW dipping Benioff-Wadati zone under the arc, magmatism was interpreted as the result of active subduction of the Ionian plate beneath Calabria (Barberi et al., 1973; Ellam et al., 1989; Francalcanci et al., 1993; Mandarano et al., 2016). On the contrary, seismicity has recently led workers to infer passive subduction of a detached slab,

with Aeolian island magmatism relating to a post-subduction extensional back-arc tectonic regime (De Astis et al., 2003, Chiarabba et al., 2008). Lines of evidence supporting a post-subduction setting include the half-ring shape of the islands and the seamounts, as appose to an arcuate chain. Also the volcanoes are situated 200-300km above the Benioff-Wadati zone, significantly higher than at many other volcanic arcs (~120km) (Gvirtzman and Nur, 1999). Finally the Aeolian Islands are erupted into thinned continental crust (~15-20 km). It appears that the magmatism of the Aeolian Islands reflects a combination of tectonic related influences, including back-arc extension and past subduction with a remnant plate present beneath the islands (Chiarabba et al., 2008). Consequently, the effusive and explosive eruptions on the Aeolian Islands have produced a large variety of products with differing magmatic associations. These range from calc-alkaline (CA), high-K calc-alkaline (HKCA), shoshonitic (SHO) and K-Series (KS) affinities (Ellam et al., 1988; Francalanci et al., 1993; Gertiser and Keller, 2000; Gioncada et al., 2003; Pecellino et al., 2013). A brief summary of the overall volcanic histories of the four studied Aeolian Islands are presented in **Table 1**.

3. Samples

3.1 Proximal eruptive units on the Aeolian Islands

Explosive volcanism in the Aeolian Islands is dominated by mid to low intensity (Strombolian, Vulcanian and sub-Plinian) eruptions, the largest of these producing approximately ~ 0.5 km^3 of pyroclastic material (Calanchi et al., 1993; De Rosa et al., 2003b; Dellino et al., 2011; Lucchi et al., 2013d). This explosive volcanism is often driven by magma mixing (Calanchi et al., 1993; De Rosa et al., 2003b; Sulpizio et al., 2008). Evidence of phreatomagmatic activity is also observed on Vulcano (De Astis et al., 1997; Lucchi et al., 2008; Dellino et al., 2011). On Stromboli hydromagmatic activity is linked with flank failure events along the Sciara del Fuoco allowing water to enter into the conduit system (Bertagnini and Landi, 1996; Giordano et al., 2008; Francalanci et al., 2013). Tephra deposits are generally characterised by a mixture of fall units from unsteady columns and flow units from small volume, short run out

pyroclastic density currents (PDC). **Table 2** summaries the eruption units of Vulcano, Lipari, Salina and Stromboli deposited during approximately the last 50 ka, in stratigraphic order, that were targeted for geochemical characterisation in this paper. Where sampling follows our own stratigraphic investigations for an individual eruption then the stratigraphic description in **Table 2** is marked by a † symbol and further details are provided in **Supplementary material 1**, otherwise the referenced published stratigraphy is followed, with sampling related to these stratigraphic investigations (also outlined in **Supplementary material 1**). **Figure 2** shows a selection of outcrop photographs of sampled stratigraphic sequences. Published ages of eruptive units have been extracted from the literature and include radiocarbon and K/Ar ages (**Table 2;** and references therein).

3.2 Distal deposits in the marine core M25/4-12 (Ionian Sea)

The marine core M25/4-12 was retrieved at a 2473 m water depth during the Meteor cruise M25/4 in 1993 with a piston corer from the Calabrian Rise (37°57'98"N; 18°11'04"E) in the Central Ionian Sea **(Fig. 1a)** (Keller et al., 1996). A continuous 1 cm resolution sampling of the core was conducted as part of a cryptotephra investigation. Sediments spanning from the top of Sapropel 1 (24-36 cm b.s.f) down to the visible Y-3 tephra at 117-118 cm b.s.f (Keller et al., 1978; Albert et al., 2015) were newly investigated for the presence of Aeolian Island derived cryptotephra layers.

4. Methods

Proximal juvenile clasts from both fall and flow tephra deposits were cleaned, dried and mounted in Streurs Epofix epoxy resin. Mounts were sectioned and polished and scanning electron microscopy was conducted to determine suitable glass locations for geochemical analysis, thus avoiding phenocrysts and microlites. The cryptotephra investigations of the sediments of Ionian Sea marine core M25/4-12 followed the procedures of Blockley et al. (2005), whilst the physical extraction of glass shards for geochemical characterisation followed the methods of Lane et al. (2014). Major and trace element micron-beam glass data

was collected using a wavelength-dispersive electron microprobe (WDS-EMPA) and Laser Ablation Inductively Coupled Mass Spectrometry (LA-ICP-MS), with the methods described in **Supplementary material 2**. The full geochemical dataset along with secondary standards run routinely with the tephra samples are available in **Supplementary material 3**.

5. Results

Glass compositions of the investigated tephra units erupted on the Aeolian Islands during approximately the last 50 ka are highly variable in their major element compositions showing CA, HKCA, SHO and KS affinities **(Fig. 3)**. Mantle normalised patterns of these glass compositions are dominated by a diagnostic subduction signature with depletions in Nb and Ta **(Fig. 4)**. The analysed chemical compositions of tephra deposits on the islands of Vulcano, Lipari, Salina and Stromboli are described below. Representative major, minor and trace element glass data for all eruption units are shown in **Tables 3** and **4,** and all geochemical data is available in **Supplementary material 3.**

5.1 Vulcano

The tephra deposits erupted on Vulcano during the last ~21 ka BP are particularly diverse, glasses ranging from basaltic trachy-andesite to rhyolite, with both SHO and KS affinities (**Fig. 3a**). The tephra units with KS glasses are the Upper Tufi di Grotte dei Rossi scoria (8.5 ka), the Palizzi A and Palizzi D layers (2.1-1.5 ka), the varicoloured Commenda Ash (918-1302), the lower Pietre Cotte (AD 1626-1727) and the darker pumice component within the mingled Upper Pietre Cotte (AD 1731-39). These glasses show significant compositional heterogeneity ranging from basaltic trachy-andesite to trachyte (**Fig. 3b**) with 53.5-61.6 wt.% SiO_2, 0.4-0.8 wt.% TiO_2, 16.2-19.4 wt.% Al_2O_3, 3.6-9.2 wt.% FeOt, 0.7-4.1 wt.% MgO, 2.0-8.0 wt.% CaO, 3.5-5.6 wt.% Na_2O, 4.3-8.3 wt.% K_2O (**Fig. 3**). Trace element concentrations are equally heterogeneous with 383-1270 ppm Sr, 117-274 ppm Zr, 16-33 ppm Nb, 928-2006 ppm Ba and 17-41 ppm Th (**Fig. 5**). Glasses display LREE enrichment relative to the

HREE (La/Yb = 27.9; **Fig. 4b**). Incompatible trace element ratios in the analysed KS glasses of Vulcano are instead largely similar (**Table 5**).

The SHO tephra units comprise the Quadrara formation (21 ka), Casa Lentia (13 ka), Palizzi B (2.1-1.5 ka) and the light pumice component of the mingled Upper Pietre Cotte (AD 1731-39) (**Fig. 3a**). These SHO glasses display even greater heterogeneity than the KS ones erupted on the island during the last ~21 ka, and range from trachy-andesite to rhyolite with 56.4-74.2 wt.% SiO_2 (**Fig. 3b**), 0.1-0.8 wt.% TiO_2 (**Fig. 5a**), 13.1-18.4 wt.% Al_2O_3, 1.8-6.8 wt.% FeO, 0.1-2.8 wt.% MgO, 0.7-8.0 wt.% CaO, 3.6-6.5 wt.% Na_2O and 4.1-8.0 wt. % K_2O (**Fig. 3a**). Incompatible trace element concentrations (e.g., 150-303 ppm Zr; 17.2-61.2 ppm Th; **Fig. 5**) and ratios observed in these SHO glasses are particularly variable (**Table 5**).

5.2 Lipari

Most of the glass compositions of the tephra units investigated on Lipari during approximately the last 50 ka have a HKCA affinity, with some straddling the boundary with the SHO series (**Fig. 3a**). The investigated eruption units from oldest to youngest include the Punta del Perciato (55-43 ka) and Falcone (43-40 ka) formations of EE 7, the Monte Guardia (24,650-27,100 cal yrs BP; Table 2) succession of EE 8, the Vallone del Gabellotto (8,430-8,730 cal yrs BP), the Monte Pilato (776 AD) and Lami (0.7 ka) successions of EE 9 (**Table 2**). These units show the following chemical variability from trachyte to rhyolite: 67.9-76.8 wt.% SiO_2, 0.01-0.36 wt.% TiO_2, 12.1-16.6 wt.% Al_2O_3, 1.0-3.3 wt.% FeO, 0.6-2.3 wt.% CaO, 2.8-4.6 wt. % Na_2O, 4.9-6.3 wt.% K_2O (**Fig. 6a**), with the rhyolitic end-member being dominant throughout all the eruptive units **(Fig. 3b).** Trace element concentrations observed in these glasses are variable and range from 7-300 ppm Sr, 32-44 ppm Y, 115-197 ppm Zr, 29- 46 ppm Nb, 3-361 ppm Ba, 31-68 ppm La (**Fig. 6b**) and 34-58 ppm Th (**Fig. 6b-e**). Incompatible trace element compositions of the rhyolitic glasses erupted on Lipari normalised to primitive mantle show pronounced depletions in Sr, Ba and Eu consistent with K-feldspar fractionation (**Fig. 4a**). Incompatible trace element ratios vary between the EE

(e.g., Nb/Th, Nb/Zr; **Table 5**), whilst the glasses show LREE enrichment relative to the HREE it is reflected in a shallow profile (La/Yb = 10 ± 3.6 [2.s.d.]) (**Fig. 4a**).

The Monte Guardia glasses show significant chemical heterogeneity through the stratigraphic succession investigated (**Fig. 7a**), subdivision in this stratigraphic succession are detailed in **Supplementary material 1**. The most heterogeneous glasses are predominantly recorded in the mingled pumices of the lower most fall deposits (U1), which have 70.2-76.8 wt.% SiO_2 and 4.9-6.3 wt.% K_2O. The overlying PDC deposits (U3) have glass compositions that lie at the more evolved end of the chemical variation seen in the underlying fall unit, indeed they are far less variable in terms of their SiO_2 (74.3-76.7 wt.%) and K_2O (5.2-6.1 wt.%), whilst the uppermost fall (U4) deposits are restricted to the most evolved compositions with high SiO_2 (75.9-76.8 wt.%) and low K_2O (5.0-5.6 wt.%). There is a clear inflection to lower K_2O in the Monte Guardia glass compositions at ca. 72-74 wt.% SiO_2. (**Fig. 6a**).

5.3 Salina

The investigated tephra deposits on Salina are associated with the Pollara activity. The sub-Plinian fall deposits of the Lower Pollara succession (26,410-27,630 cal yrs BP; **Table 2**) have glasses that straddle the CA/HKCA boundary **(Fig. 3a).** Glass analysis of the opening scoria fall were not successfully obtained owing to the absence of matrix glass within these particularly crystal rich clasts. The Lower Pollara pumice fall deposits were sampled in two localities, Valdicheiesa on Salina and the 'Key Bed' layer on recorded on Lipari (**Fig. 1; Table 2**) and show both white and grey pumice components reflected in consistent heterogeneity shown in their glass compositions (68.2-75.1 wt.% SiO_2; 1.7-4.1 wt.% CaO and 2.6-3.7 wt.% K_2O; **Fig. 3a**). Glass compositions range from dacitic to rhyolitic in composition (**Fig. 3b**). The more evolved compositions demonstrate a subtle inflection towards lower K_2O concentrations (**Fig. 7a**). Incompatible trace element concentrations show some variation, for instance 107-143 ppm Zr, 10.7-13.9 ppm Nb and 10.0-13.3 ppm Th

(**Fig. 7**). In the absence of K-feldspar the Ba concentrations of the glasses extend to elevated concentrations (836-1010 ppm Ba; **Fig 7**). Incompatible trace element ratios observed in the Lower Pollara glasses are typically consistent (**Table 5**), and they display LREE enrichment relative to the HREE (La/Yb = 18.6 ± 2.9 [2 s.d.]).

The PDC deposits of the Upper Pollara succession (15,000-16,090 cal yrs BP; **Table 2**); were sampled from five successive eruption units (ERU) recognised by Sulpizio et al. (2008) (**Supplementary material 1**). All analysed glasses are rhyolites with a HKCA affinity (**Fig. 3**). Considerable geochemical variation is observed within these glasses (71.4-77.6 wt.% SiO_2; 0.9-3.0 wt.% CaO and 3.4-4.4 wt.% K_2O) which is consistent with the white and grey banding observed in most pumices. Of the five compositionally overlapping eruption units, the most evolved glasses (e.g., highest SiO_2 and lowest CaO) are seen in ERU3 and ERU4, whilst the least evolved ones are in ERU1 and ERU5 (e.g., lower SiO_2 and higher CaO; **Fig. 7**). Stratigraphic differences are observed in the incompatible trace element concentrations, the most elevated concentrations were seen in the glasses of ERU3 and ERU4 (122-139 ppm Zr; 18.0-19.6 ppm Th), whilst the lowest is seen in underlying ERU1 and ERU2 (101-114 ppm Zr; 13.1-17.4 ppm Th) (**Fig. 8**). Incompatible trace element ratios observed in the glasses are typically consistent (**Table 5**), and the glasses display LREE enrichment relative to the HREE (La/Yb = 21.2±3.9 [2 s.d.]).

5.4 Stromboli

The oldest tephra deposits investigated on Stromboli are pumice fall deposits related to the Upper Vancori activity (**Table 2**). Three eruptive units were distinguished (Supplementary material 1). All glasses are classified as Trachytic **(Fig. 3b)** with a clear SHO (63.2-65.4 wt.% SiO_2; 5.3-5.8 wt.% K_2O) affinity **(Fig. 3a).** The basal fall, unit 1, (Fig. 2o) has more evolved glass compositions (e.g., 65.1 ± 0.4 wt.% SiO_2; 0.9 ± 0.1 wt.% MgO; 2.5 ± 0.2 wt.% CaO [2.s.d]) compared to the upper pumice fall, unit 3 (e.g., 63.7 ± 0.6 wt.% SiO_2; 1.1 ± 0.1 wt.% MgO; 3.0 ± 0.2 wt.% CaO [2.s.d]; **Fig. 8b**). Incompatible trace element concentrations

and ratios are consistent between the two eruption units **(Table 5)**. Glasses show LREE enrichment relative to HREE (La/Yb = 18.8 ± 2.5 [2 s.d.] (**Fig. 4**)). Some heterogeneity is observed in the absolute trace element concentrations of the entire analysed Upper Vancori suite of glasses consistent with major element variability (e.g., 261-327 ppm Zr; 27-35 ppm Th).

The so-called Holocene Secche di Lazzaro hydromagmatic tephra deposits were sampled from two outcrops, one along the Semaforo Labronzo track in northern Stromboli and (**Fig. 1b;** Loc. 17) and the second near the COA (Advanced Operation Centre (Fig. 1b; Loc. 18), to complement the glass data presented from the Secche di Lazzaro type locality near Gionastra in the south-western sector of the island (Petrone et al., 2008). Overall glasses analysed are heterogeneous ranging from trachy-andesites to trachytes **(Fig. 3b),** and all with a KS (57.5-60.2 wt.% SiO_2; 6.4-7.1 wt.% K_2O) affinity **(Fig. 3a)**. The least evolved, trachy-andesitic glasses (57.8 ± 0.4 SiO_2; 6.5 ± 0.4 wt.% FeOt; 4.6 ± 0.2 wt.% CaO [2 s.d.]) are observed in the lowermost scoria fall unit (U2) of the Semaforo Labronzo outcrop (**Fig. 1;** Loc. 17). Pumices from the Semaforo Labronzo lahar deposit (U5) and those from the COA outcrop (U3 and U4) show a more evolved, homogeneous, trachytic glass composition (59.5 ± 0.7 wt.% SiO_2; 5.6 ± 0.5 wt.% FeOt; 4.0 ± 0.4 wt.% CaO [2 s.d.]; **Fig. 8**). Incompatible trace element concentrations observed in the glasses of both the scoria and pumices are overlapping, but significant variation is observed throughout all the glasses investigated (e.g., 253-339 ppm Zr; 28.1- 35.6 ppm Th). Vanadium is the only trace element to significantly differ between the scoria (172.6 ± 9.5 [2.s.d]) and pumices (136.4 ± 19.4 [2 s.d.]) glasses. Barium concentrations are particularly elevated in the analysed glasses as it continues to behave incompatibly (e.g., 1958-2490 ppm Ba). The incompatible trace element ratio of the scoria and pumices are consistent and all glasses show LREE enrichment relative to HREE (**Table 5**).

6: Discussion: Tephrochronological implications

6.1 Diagnostic Island to Island geochemical variations:

Rhyolitic glass compositions are common in the tephra deposits of the Aeolian Islands during the investigated time span, and the products of Lipari, Salina and Vulcano can be successfully separated using SiO_2 vs K_2O **(Fig. 3a)**, other key discriminators are observed at a major element level. CaO vs FeO is useful for distinguishing the deposits of the different islands with the exception of Vulcano and Stromboli. Salina rhyolites show higher CaO at overlapping FeOt concentrations when compared to the Lipari (**Fig., 7b**) and Vulcano glasses. Furthermore the Lipari rhyolitic glasses extend to lower CaO and FeOt when contrasted with those of Vulcano (**Supplementary material 1**).

Trace element concentrations within the glasses offer further means to distinguish the rhyolitic tephra units erupted on Lipari, Vulcano and Salina during the last ~ 50 ka. Mantle normalised trace element profiles of glasses can offer a useful first order discriminator to help determine the provenance of a distal tephra. Dacitic to rhyolitic glasses erupted on Salina show significantly lower levels of overall incompatible trace element enrichment when compared to the rhyolitic glasses of both Lipari and Vulcano **(Fig. 4a)**. K-feldspar fractionation is assumed as responsible for strong negative anomalies at Ba, Sr and Eu within the mantle-normalised profiles of glasses erupted on Lipari. Whilst less pronounced, these depletions are also observed in the Vulcano rhyolites. K-feldspar is instead absent in the mineral assemblage of the investigated Salina tephra deposits, and consequently no such depletions are observed in the corresponding glass compositions. Indeed, Ba continues to behave incompatibly in the highly silicic melts of Salina (ca. 70-76 wt.% SiO_2). Ba enriched rhyolitic glasses are unlikely to relate to explosive activity on Lipari or Vulcano.

SHO and KS explosive eruptive deposits are observed on Vulcano and Stromboli during the last 21 ka and they share broadly overlapping major element chemistries (**Fig. 3**). Fortunately some diagnostic features can be used to help assign provenance to distal tephra originating from these two volcanic islands. When comparing Vulcano or Stromboli proximal

glasses with either a SHO or KS affinity, the TiO_2 content is crucial for distinguishing the products of their products. At any given silica content, the Stromboli glasses contain significantly higher TiO_2 than the glasses erupted on Vulcano (**Fig. 5a**). Trace element concentrations presented here are particularly indicative of different petrological processes operating beneath Vulcano and Stromboli and provide an essential discriminatory potential. Mantle-normalised profiles of proximal glasses erupted on the two islands clearly demonstrate that the Vulcano glasses are more depleted in Nb-Ta and Zr than the Stromboli glasses **(Fig. 4b)**. Subsequently, the High Field Strength element ratios are helpful for deciphering the provenance of unknown tephra possibly sourced from Vulcano or Stromboli. The Nb/Th ratio is particularly crucial, with Stromboli glasses showing more elevated values than those of Vulcano **(Fig. 5b; Table 5)**. Zr/Th is also a useful ratio for discriminating the younger (Holocene) KS activities of the two islands (**Table 5**). For instance La Fossa cone on Vulcano have significantly lower values than those observed in the Secche di Lazzaro glasses of Stromboli.

6.2 Island specific geochemical variation (Lipari)

In the following section we explore the use of major, minor and trace element glass chemistry to decipher successive eruptions from a single volcanic source. In this section we focus upon the geochemical variability of the eruptive products of Lipari spanning approximately the last 50 ka. Further descriptions of diagnostic geochemical variation observed between successive eruptions on Vulcano and Salina are presented in **Supplementary material 4** according to the units described in **Table 2**.

Lipari has erupted near identical trachytic to rhyolitic magma compositions during approximately the last 50 ka with dominant HKCA rhyolites (~75 wt. % SiO_2) and overlapping major element compositions. This is highly problematic for distal tephrochronology. However our geochemical data reveals that concentrations of certain trace elements (e.g., the LREE and Th) are particularly useful for distinguishing the proximal glasses erupted on Lipari.

Clear chemostratigraphic trends through the successive eruptive deposits **(Fig. 6)**. Temporally each new eruptive epoch taps magmas which become more enriched in Th **(Fig. 6c).** This offers significant potential to constrain the relative stratigraphic position and age of Lipari-derived distal tephra deposits recorded in the volcanic stratigraphies of the neighbouring Aeolian Islands or further afield in sedimentary archives where the stratigraphy or chronology may be less well constrained. Hereafter we assess the observed geochemical features which can aid in deciphering the eruptive products spanning the last three EE (7 to 9) of the island.

6.2.1 Punta del Perciato and Falcone formations (EE 7)

The Punta del Perciato and Falcone units are stratigraphically well distinguished (Forni et al., 2013; and references therein). Punta del Perciato is younger than the so-called Ischia tephra (dated to 55 ka following it correlation to the Monte Epomeo Green Tuff of Ischia; Tomlinson et al., 2014) and the Falcone unit dated at 40-43 ka. These two units are separated by a Brown tuff ash accumulation which represents a period of quiescence on the island of Lipari **(Fig. 2a)**. The main geochemical means for distinguishing these two stratigraphic units is through the observed compositional heterogeneity. The older Punta del Perciato deposits are very homogeneous HKCA rhyolites, whilst the younger Falcone ones have a greater range in silica content, displaying trachytic to rhyolitic glass compositions (**Fig. 6a**). The more variable compositions in the Falcone deposits are consistent with the presence of both grey and white pumices which is likely to evidence magma mixing. Trace element concentrations of the glasses are largely indistinguishable, although the Falcone glass data show more variation compared to the Punta del Perciato ones owing to the presence of lower silica rhyolites. The most useful elements for distinguishing these tephra deposits based on absolute concentrations appear to be La and Ce, with subtly more elevated values observed in the rhyolitic glasses of the Falcone tephra relative to the older Punta del Perciato **(Fig. 6e)**.

6.2.2 Monte Guardia succession (EE 8)

The Monte Guardia succession (EE 8) occurs stratigraphically above the Falcone Formation on Lipari and is separated by a Brown Tuff accumulation representing a period of quiescence on Lipari (**Fig. 2a**). The Monte Guardia eruption is dated within a 24,650-27,100 cal yrs BP time-stratigraphic interval, derived from calibrated radiocarbon ages of charcoal from the Brown Tuffs deposits directly above and below the Monte Guardia deposits (Lucchi et al., 2013b; Forni et al., 2013; and reference therein; **Table 2 and Supplementary material 2**). The Monte Guardia glasses show the most significant chemical heterogeneity if compared to the other sampled pyroclastic units erupted on the island of Lipari during the last 50 ka. Whilst their silica variation is consistent with the glasses of the underlying Falcone formation (**Fig. 6a**), the higher SiO_2 rhyolitic end-member of the Monte Guardia glasses present significantly more K_2O variation than those of the Falcone. A key diagnostic feature of the Monte Guardia succession is the compositional variability observed through the stratigraphy (De Rosa et al., 2003b). At a major element level the most compositional heterogeneity is observed in the lowermost fall units where SiO_2 and K_2O range from 70-76 wt.% and 4.9-6.1 wt.% respectively (Unit 1). The overlying PDC deposits and the uppermost fall deposits are instead restricted to the most silicic compositions (ca. 74-76 wt.% SiO_2 [Units 3 and 4]). The chemostratigraphy of the Monte Guardia succession was related to the emptying of a reversely zoned magma system, where the least evolved compositions are deposited during the earlier phases of the eruption (De Rosa et al., 2003b). Importantly the lowermost fall unit displays the full compositional range of the Monte Guardia succession consistent with the physical evidence of magma mingling observed in the banded white and grey pumices. Furthermore the least evolved glass compositions of this eruption are never found exclusively within the stratigraphy and are always accompanied by the higher SiO_2 (rhyolitic) white pumice component. Incompatible trace element concentrations observed in the Monte Guardia glasses are highly variable (e.g., Th 34.2-43.1 ppm; **Fig. 6c)** consistent with the major element variation.

Distinguishing the Monte Guardia glasses from those of the older stratigraphic units of EE 7 on Lipari (Punta del Perciato and Falcone) can be achieved using a combination of diagnostic major and trace element features. The least evolved Monte Guardia glasses show an higher K_2O content than the Falcone glasses, whilst the most silicic Monte Guardia glasses (>75 wt.% SiO_2) extend to much lower K_2O **(Fig. 6a)** and higher Na_2O concentrations than the Punta del Perciato and Falcone glasses. Furthermore Monte Guardia glasses have a much wider range in Th concentrations, extending to more enriched concentrations than those in the Punta del Perciato and Falcone glasses **(Fig. 6c)**.

6.2.3 Vallone del Gabellotto (EE 9)

Following the Monte Guardia eruption another period of quiescence is observed on Lipari, associated with a shift in the activity to the NE of the island (Lucchi et al., 2010). Brown tuff deposits are deposited in the intervening period, together with some deposits of local origin. In particular the Vallone Canneto Dentro pyroclastic succession and the *l3* layer have HKCA rhyolitic pumices (Lucchi et al., 2010). These are stratigraphically constrained as being younger than the Monte Guardia and older than the Vallone del Gabellotto. They were not analysed on this study due to their limit dispersal and scarce outcrop exposure.

The Vallone del Gabellotto succession is the result of an explosive eruption in the NE sector of Lipari. Its most widely accepted age is that of the marine equivalent E-1 which lies in Sapropel 1 at 8,430-8,730 cal yrs BP (7,770 ± 40 ^{14}C yrs BP; **Table 2**). This succession is dominated by pumiceous PDC units with a very homogeneous HKCA rhyolitic glass composition and no chemostratigraphic variation (**Fig. 6**). In addition to a different stratigraphic position, the Vallone del Gabellotto glasses are easily distinguished from those of the Monte Guardia given their consistently lower SiO_2 contents, and the absence of magma mixing. Moreover, where SiO_2 does overlap, the Monte Guardia glasses show more elevated K_2O (Fig. 6a). The Vallone del Gabellotto glasses are enriched in a number of trace

elements when compared to those of the Monte Guardia, and include Zr, LREE and Th (**Fig. 6**), as reflected in differing incompatible trace element ratios (**Table 5**).

6.2.4 Monte Pilato and Lami successions (EE 9)

Following the Vallone del Gabellotto activity a period of quiescence is recognised on Lipari until historical times, with the eruption of the Monte Pilato dated to 776 cal AD ([14]C 1,241 ± 31 yrs BP; **Table 2**). This eruption produced a succession of HKCA rhyolitic fall deposits that are difficult to distinguish at a major element level from the Vallone del Gabellotto deposits. Stratigraphically two eruptive phases in Monte Pilato activity (Monte Pilato 1 [lower] and Monte Pilato 2 [upper]) were recognised by Albert et al. (2012), as supported by subtle stratigraphic and chemical differences. The lower Monte Pilato 1 glasses have a dominance of higher SiO_2 glasses relative to Monte Pilato 2 and the older Vallone del Gabellotto succession (**Fig. 6a**). Interestingly, the subtly more silica rich Monte Pilato 1 glasses show lower levels of incompatible trace element enrichment relative to the Monte Pilato 2 glasses, which are instead consistent with the Vallone del Gabellotto glasses **(Fig. 6c)**. Consequently, distinguishing the lower Monte Pilato 1 glasses from those of the Vallone del Gabellotto is particularly difficult and relies on the subtly elevated SiO_2 contents in the former, which is ultimately within analytical error. The upper Monte Pilato 2 glasses show higher levels of trace element enrichment when contrasted with the Monte Pilato 1 and Vallone del Gabellotto glasses, a useful discriminatory feature.

The Lami pyroclastic succession is localised along the southern flank of the Monte Pilato cone. Its relative timing within the context of the final explosive activities on Lipari is still contested. Davì et al. (2011) presented a detailed stratigraphic investigation into the Lami succession and considered this to be part of the main Monte Pilato succession, and this coeval with the sampled Monte Pilato fall units. Alternatively, Forni et al. (2013) place the Lami succession as stratigraphically above the Monte Pilato, and instead time-equivalent with the younger Rocche Rosse coulee (1220 AD). This would be consistent with the age of

0.70 ± 0.17 ka for the Lami formation produced by Bigazzi et al. (2003). Accordingly, the Lami pyroclastic succession, along with the Rocche Rosse coulee and pyroclastics, are representative of the most recent eruptive activity of Lipari.

Chemical differences between the Lami glasses and those of Monte Pilato might support a time-stratigraphic separation. Indeed, the Lami glasses are subtly less evolved, with lower SiO_2 and higher K_2O content compared to the Monte Pilato fall deposits. Furthermore the Lami glasses have LREE (**Fig. 6b**) and Th (**Fig. 6c**) contents that are more elevated than those of the MP, and they are instead consistent with data for the younger Rocche Rosse lava flow (**Fig. 6b**). Clearly, the presence of higher levels of incompatible element enrichment, and in particular the elevated LREE concentrations, appears diagnostic of the most recent explosive activity on the island.

6.3 Spatial proximal geochemical variations (Stromboli)

The so-called Secche di Lazzaro deposits are recognised at localities around the island. These deposits were related to hydromagmatic eruptions closely linked to a collapse of the Sciara Del Fuoco (Bertagnini and Landi, 1996). Volcanic glass from the type locality Secche di Lazzaro sequence, recognised in the south-western sector of the island, have been characterised by Petrone et al. (2009) along with samples from two outcrops located on the north-eastern side, which are also the focus of this work. The complexity of the Secche di Lazzaro sequences is manifested in the different interpretations present in the literature with the deposits interpreted as a single (Bertagnini and Landi, 1996; Giordano et al., 2008), or two (Porreca et al., 2006) eruptive events based on deposit analyses, where these sequences have been subsequently considered the result of the depressurisation of two shallow magma bodies with subtly differing compositions (Petrone et al., 2009). More recently, Francalanci et al. (2013), have suggested the spatial variability in chemistry and differences in the time-stratigraphic position of the deposits around the island indicate three different hydromagmatic pyroclastic successions in the southern (Secche di Lazzaro; type

locality), north-eastern (Semaforo Nuovo Formation) and northern (Semaforo Labronzo Formation) sectors of the island. These authors suggest all three eruptions are related to successive failures of the Sciara del Fuoco spanning the period of 12-4 ka.

The glasses of samples analysed here all share a KS affinity (**Fig. 3a**). Geochemically, these glasses compositionally vary spatially between different localities on the island, and these variations are largely restricted to major elements (**Fig. 8**). Indeed, incompatible trace element concentrations (excluding vanadium) and ratios are indistinguishable between the different localities (**Table 5**). The lowermost and least evolved scoriaeous deposits from the Semaforo Labronzo outcrop (Locality 17; **Fig. 1**), chemically correspond with the glasses of the lowermost unit (UA) of the type locality sequence (**Fig. 8**; Petrone et al., 2008), and are not identified in the sequence near to the COA investigated here (Locality 18; **Fig. 1**) (**Fig. 8**). Yet the more evolved compositions of the COA deposits are also seen entrained within the upper lahar deposit of the Semaforo Labronzo sequence, but also in the intermediate UB of the type locality Secche di Lazzaro (**Fig. 8**).

The spatial chemical variations observed in this work between the Secche di Lazzaro deposits can be either used to interpret that the deposits are the result of different eruptions, in agreement with the findings of Francalanci et al. (2013), or suggest a possible intra-eruptive variability in the same eruption. Our current chemical dataset is however not conclusive in elucidating these two possibilities. While some chemical heterogeneities are observed, all the studied sequences show in part some shared chemical affinity, this possibly indicates that the sequences are incomplete at individual outcrops. Moreover, it is difficult to reconcile that these three eruptions might span a large time frame (12-4 ka) but show the same chemical range, this might instead then favour a hypothesis of a complex, but single eruption. Further detailed chemical analysis of volcanic glasses, in particular from those of the Secche di Lazzaro type locality (south-western Stromboli), but at additional localities on the island, and proximal-distal correlations could help to better examine the proposed time-stratigraphic reconstruction. Indeed, nearby marine records may offer the

opportunity to stratigraphically and chemically assess the relative age reconstruction of these eruptive deposits on the island, which remains relatively uncertain, with only the Secche di Lazzaro type locality deposits radiocarbon dated at 7 ka cal BP (Francalanci et al., 2013).

6.4 Aeolian Islands- proximal-distal tephra correlations

In the following sections we apply our proximal glass geochemical datasets to assess the provenance of distal tephra layers associated with explosive eruptions on the Aeolian Islands. This includes marker beds sampled from the neighbouring islands and also layers recorded in distal marine and lacustrine archives of the central Mediterranean. Both new and published data are used, although we acknowledge that interpretations following comparisons with literature data should be taken with some caution owing to offsets associated with differing analytical conditions. Due to similar major element glass chemistries of the products of Vulcano and Stromboli the distal deposits sourcing from these volcanoes are discussed together.

6.4.1 Vulcano and Stromboli

Due to similar major element glass chemistries of the products of Vulcano and Stromboli the distal deposits sourcing from these volcanoes are discussed together. They are grouped together according to two time-stratigraphic intervals: 1) pre-Holocene period, comprising products older than 10 ka; (2) Holocene period, comprising products erupted during the last 10 ka.

6.4.1.1 Pre-Holocene (>10ka)

The marine tephra T1657cm (34,064-35,693 cal yrs BP; Matthews et al., 2015) reported in the southern Adriatic core SA-03-11 was tentatively correlated to activity on the island of Vulcano (Matthews et al., 2015) and lies stratigraphically below the Lipari-derived E-11 tephra (discussed below). Tephra T1657cm is older than any Vulcano tephra units

investigated here, and slightly less evolved. It clearly lies on the same SiO_2 vs TiO_2 trend as all the analysed proximal Vulcano glasses, and thus would support the existing interpretation that it represents distal ash fall from explosive activity on Vulcano **(Fig. 5a)**. Tephra T1657cm presence in the southern Adriatic demonstrates long distance ash dispersal (> 400 km) associated with a mafic eruption on the island. Whilst compositionally T1657cm is less evolved than the published data, it might still be envisaged that this ash dispersal is linked to phreatomagmatic activity on Vulcano which is thought to have produced the so-called intermediate Brown Tuffs (**Fig. 3**) recorded on most of the Aeolian archipelago during the 56-27 ka time interval (Lucchi et al., 2008; 2013b).

Distal occurrences of the sub-Plinian Quadrara deposits (21 ka; **Table 2**) originating in the southern sector of Vulcano are reported on Capo Milazzo (Morche, 1988) and more tentatively on Panarea (EL4; De Rita et al., 2008), whilst further afield in the sediments of Lago Pergusa, Sicily (T-3; Narcisi, 2002). Our new chemical glass data for the Capo Milazzo pumices (**Supplementary material 3**) support the proposed correlation of Morche (1988) based on diagnostic major and trace elements characteristics (**Fig. 5; 8)** The presence of Quadara deposits on Capo Milazzo, 20 km, south of Vulcano, coupled with its absence further north on the island, supports a dominant southerly dispersal for this eruption. Whilst instead the trachytic EL4 pumices outcropping on Panarea **(Supplementary material 3)** have glass compositions inconsistent with those of the Quadrara deposits, with crucially too high TiO_2 content when compared to the trachytic Quadrara endmember **(Fig. 5a)**. Thus our glass data enable us to exclude a provenance of the EL4 pumices from Vulcano. In many respects the EL4 glasses appear more consistent with the trends observed in our Stromboli data-set (**Fig. 5a**). Indeed, incompatible trace element compositions are also more consistent with Stromboli glasses (**Fig. 5b-c**). Whilst a provenance from Stromboli cannot be ruled out given the compositional similarities, no obvious proximally recorded units are known. Therefore a more proximal source for the EL4 pumices might be suggested. Indeed the EL4 pumices appear to correspond to the Drauto Formation of Lucchi et al. (2013d)

which is related to fall originating from explosive activity located around the islets east of Panarea, and this might explain the chemical similarities with the Stromboli glasses. The T-3 tephra recorded in the lacustrine sediments of Lago Pergusa, Sicily (Narcisi, 2002) occurs stratigraphically below the Monte Guardia. Thus a correlation to the Quadrara tephra of Vulcano is not possible, owing to a reversed relative stratigraphic ordering (Keller, 1980a; De Astis et al., 2013a). Equally problematic is that the K_2O contents of the T-3 tephra are significantly more elevated than those seen in the proximal Quadrara glasses (**Fig. 3a**). Comparing the T-3 tephra with our proximal glass data-set does re-affirm that it is likely to derive from an eruption of Vulcano **(Fig 5a)**, but it is prior to Quadrara eruption.

The SHO tephra I-I-a bottom is reported by Insinga et al. (2014) in the Ionian Sea core KC01B at 18.7 ka. By comparing the glass compositions of this tephra to our proximal data-set it supports an origin from explosive activity on Vulcano (Fig. 5a). The age of the tephra would mean it is likely to relate to explosive activity prior to the La Fossa cone. Zirconium and Th concentrations of the distal tephra are indeed consistent with the activity older than La Fossa (**Fig. 5c**). A potential correlation is with one of the phreatomagmatic eruptions that produced the so-called Upper Brown Tuffs and dated to between 24-8 ka (Lucch et al., 2008; 2013b). However, currently available major element glass data for the Upper Brown Tuffs are more evolved than the distal tephra (**Fig. 3**).

The trachytic tephra layers KET8003-154cm (13.9 ka) and KET8011-94cm (11.9 ka) (**Fig. 3**) also reported from the marine sediments of the southern Tyrrhenian Sea (Paterne et al. 1988) clearly conform to the SiO_2 vs TiO_2 trends observed in the Vulcano glasses from the present study **(Fig. 5a)**. A geochemical re-investigation of KET8011-94cm and KET8003-154cm could be useful in assessing precise proximal correlations to eruptive deposits on Vulcano.

6.4.1.2 Holocene (>10ka)

TIR2000-50cm recorded in the Marsili basin, southern Tyrrhenian Sea, was initially considered a distal deposit associated with the phreatomagmatic Secche di Lazzaro eruption of Stromboli (Di Roberto et al., 2008). However, the TiO_2 content (**Fig. 5a**) and diagnostic Nb/Th and Zr/Th ratios of the glasses suggest that Vulcano is the likely source (**Fig. 5b-c**). Our major and trace element glass data suggest a geochemical overlap with the Palizzi A activity (2.1 ka; **Table 2**), however, there is an significant age discrepancy, as TIR2000-50 is stratigraphically below TIR2000-30cm which is correlated to the AP1-3 eruptions of Somma-Vesuvius dated between 3.4 and 2.7 ka (Di Roberto et al., 2008; references therein). TIR2000-50cm is broadly consistent with the glass compositions of the Upper Brown Tuffs reported by Lucchi et al. (2008) and sampled from the Vulcano (**Fig. 3**), this correlation requires further investigations.

The layer KET8011-35cm (5.7 ka) recorded in the southern Tyrrhenian (Paterne et al., 1988) shows a more elevated TiO_2 content consistent with an origin from Stromboli rather than Vulcano **(Fig. 6a).** Given this clear affinity to Stromboli and its age we tentatively propose a correlation of the distal layer to the Secche di Lazzaro deposits (5-7 ka; **Table 2**), although given the slight chemical offsets, and proximal complexities, a re-investigation of this distal tephra is necessary to assess a more precise proximal correlation. The tephra layer KET8003-0cm from the southern Tyrrhenian Sea (Paterne et al., 1988), is clearly derived from more recent activity on Vulcano (**Fig. 6a**), although new chemical analysis of the distal tephra is required to establish a precise correlation with the compositionally similar KS proximal units analysed.

6.4.2 Lipari

6.4.2.1 Lipari – E-11 correlation

The oldest distal HKCA rhyolitic tephra attributed to explosive activity on Lipari is the Tyrrhenian Sea marine tephra E-11 identified by Paterne et al. (1988) in the deep sea core KET8003 (**Fig. 1a**). The tephra is dated to 37.7 ka and occurs directly above the 40 ka BP

Campanian Ignimbrite (Y-5/C-13; De Vivo et al., 2001). More E-11 correlatives have been recently identified in Ionian and Adriatic Sea marine records again above the Campanian Ignimbrite (Insinga et al., 2014; Matthews et al., 2015). The I-2 tephra (Ionian Sea; KC01B) is dated to 34.1 ka (Insinga et al., 2014) and the T1535 tephra (Adriatic Sea; SA03-11) has a ^{14}C modelled age of 33,711-35,163 cal yrs BP (Matthews et al., 2015). These ages are approximately consistent with that of the E-11 tephra. The major element data available in the literature for the E-11 are compared here to our new proximal glass data sets **(Fig. 9)**.

This unequivocally demonstrates that the E-11 and correlatives originate from the island of Lipari. Based on its age, the E-11 tephra should be initially considered in the context of the Punta del Perciato or the Falcone explosive activities (being significantly older than Monte Guardia). However, our geochemical data for the Punta del Perciato and Falcone deposits are inconsistent with the glass compositions of the distal E-11 tephra. Indeed, at overlapping SiO_2 contents the proximal Punta del Perciato and Falcone glasses show consistently more elevated K_2O than the E-11 and correlatives (**Fig. 9**). In addition to compositional inconsistencies, the Punta del Perciato (56-43 ka) and the Falcone (43-40 ka) formations are likely to chronologically predate the Campanian Ignimbrite, whilst the E-11 tephra overlies the corresponding tephra in all reported cores. Interestingly, the most silicic Monte Guardia samples in our dataset offer a better geochemical match for the E-11 tephra **(Fig. 9)**, even if a correlation is entirely precluded by a time-stratigraphic discrepancy considering that the Monte Guardia eruption is dated at 24,650-27,100 cal yrs BP **(Table 2)**.

This presents an interesting inconsistency between the proximal and distal tephrostratigraphic archives. Proximally on Lipari there is evidence of a.15 ka long period of quiescence between the Falcone eruption and renewal of activity and the Monte Guardia (Lucchi et al., 2010, Forni et al., 2013), whilst distally a tephra layer evidences an eruption on Lipari occurred at 34-38 ka. A possible scenario is that the sub-Plinian activity of Monte Guardia has buried or destroyed the proximal evidence of another slightly older explosive eruption which occurred after the Falcone eruption.

6.4.2.2 Monte Guardia - distal correlations

The Monte Guardia eruptive deposits are identified in medial-distal localities across the Aeolian Islands including Salina, Vulcano and Panarea (Lucchi et al., 2007; 2008; De Rita et al., 2008; Lucchi et al., 2013b). In this contribution we present new glass data from southern Vulcano, near Gelso (**Supplementary material 3**), where stratigraphic investigations by Lucchi et al. (2010, 2013b) recognised the Monte Guardia PDC deposits. This mid-distal locality is characterised by the dominance of white pumices, with the grey pumice component seen more proximally on Lipari being almost absent. Glasses from the Gelso locality match the most evolved component of the Monte Guardia investigated on Lipari, with $SiO_2 > 75$ wt.% and the lowest K_2O contents in the chemical variation observed proximally within the Monte Guardia succession (**Fig. 9a**). Incompatible trace element contents of the Gelso glasses are consistent with the Monte Guardia deposits on Lipari, and can be distinguished from those of older Falcone and Punta del Perciato (**Fig. 9b**). Thus geochemical evidence presented here supports the interpretation that the Gelso layer is the mid-distal equivalent of Monte Guardia.

More distally Monte Guardia has been identified by Narcisi (2002) labelled as T2 in the sediments of Lago di Pergusa, Sicily (**Fig.1a**). This tephra is broadly consistent with the Monte Guardia proximal glasses based on most major elements, although some average compositions show SiO_2 extending to subtly more elevated values and lower K_2O (**Fig. 9a**). This most likely reflects subtle analytical differences. Chronologically the T-2 tephra is constrained between 23,555 and 25,860 cal yrs BP in the sediments of Lago di Pergusa (Narcisi, 2002), which is consistent with the 24,650-27,100 cal yrs BP age of Monte Guardia on Lipari (**Table 2**). The occurrence of Monte Guardia on Vulcano and Sicily is indicative of a large southern dispersal from a vent location in the southern sector of the island of Lipari, coupled with a northern dispersal consistent with our sampling on Lipari and the occurrence of tephra layers on Salina and Panarea (Lucchi et al., 2013b). This large dispersal area make the Monte Guardia tephra a very useful stratigraphic marker for the Aeolian Islands

volcanic stratigraphies, the paucity of tephra layers from this eruption in the Tyrrhenian deep sea cores might suggest a limit to the northern extent of ash dispersal, whilst its presence in Lago di Pergusa, Sicily, clearly testifies a more extended southern ash dispersal.

More recently, Caron et al. (2012) reported the Monte Guardia tephra in the northern Ionian Sea, within marine core MD90-918 at a depth of 820cm **(Fig. 1a)**. However, the layer has a marine reservoir corrected ^{14}C age of 19,190-19,735 cal yrs BP (16,610 ± 70 ^{14}C yrs BP; Caron et al., 2012), which is not consistent with the Monte Guardia age on Lipari (**Table 2**). Our proximal investigations confirm doubt over a correlation of this tephra to the Monte Guardia eruption. The trachy-rhyolitic glasses of MD90-918-980cm are most similar to the least evolved glasses produced on Lipari during the last 50 ka (Fig. 10a), but they are less evolved than the least evolved glasses of the Monte Guardia succession. This is in contrast to the other medial and distal occurrences of the Monte Guardia which are all dominated by the most felsic rhyolitic (>75.% SiO_2) glass compositions (**Fig. 9a**). Proximally, the less evolved compositions, associated with the grey pumices, are not found exclusively in the eruptive deposits of the Monte Guardia eruption, which is inconsistent with tephra MD90-918-980cm. This evidence suggests that MD90-918-820cm is the distal equivalent of an eruption on Lipari that occurred between the Monte Guardia and Vallone del Gabellotto activities. Possible proximal counterparts are the Vallone Canneto Dentro pyroclastic deposits or the the l3 layer recognised by Forni et al. (2013) in the time-stratigraphic interval corresponding to the age of MD90-918-980cm.

6.4.2.3 Vallone del Gabellotto - distal correlations (E-1)

The Vallone del Gabellotto succession is considered a widespread stratigraphic marker within the Aeolian Islands, outcropping on Vulcano, Panarea and Stromboli (Lucchi et al., 2007; 2008; 2013b; 2013d; De Astis et al., 2013; Francalanci et al., 2013). Beyond these terrestrial outcrops, Vallone del Gabellotto is related to the E-1 marine tephra recognised in the early-Holocene Sapropel sediments of the central Mediterranean including records from

the Tyrrhenian, Adriatic and Ionian Seas (Paterne et al., 1988; Siani et al., 2004; Caron et al., 2012). Here we present evidence for a new Vallone del Gabellotto cryptotephra recorded in the sediments of the more southerly Ionian Sea. Within the marine core M25/4-12 (**Fig. 1a**) at a depth of 28 cm b.s.f. in the middle of Sapropel 1 a peak of 2037 HKCA rhyolitic shards/per gram of dried sediment were discovered (Albert, 2012). These glasses display major and trace element compositions that are consistent with the more homogeneous compositions of the proximal Vallone del Gabellotto glasses **(Fig. 10)**, particularly when contrasted to the more chemically diverse and younger Monte Pilato and Lami successions on the island **(Fig. 10)**. Both stratigraphically and geochemically the correlation is secure, meaning that the distal age of tephra M25/4-12-28cm with Vallone del Gabellotto/E-1 is secure. This means the distal age of the E-1 (8,430-8,730 cal yrs BP; **Table 2**) can be imported into the marine core M25/4-12 and thus provides a new chronological datum to this record.

Interestingly, at a depth of 44 cm within the same core another HKCA rhyolitic cryptotephra layer was also identified with a peak of 234 HKCA rhyolitic shards per gram of dried sediment (Albert, 2012). The major element composition of this layer is identical to that of the Vallone del Gabellotto in the same core. However, at a trace element level, its glasses showed subtle differences in their LREE concentrations relative to those of the Vallone del Gabellotto, with lower LREE concentrations most noticeably in La and Ce **(Fig. 10 c-d).**

Stratigraphically the cryptotephra M25/4-12-44cm falls is older than the Vallone del Gabellotto and falls in the Late-glacial period of the record based on the oxygen isotope stratigraphy (Negri et al., 1999). Potential correlatives on Lipari would include units occurring stratigraphically below the Vallone del Gabellotto, which are the Vallone Canneto Dentro pyroclastics or the l3 layer of Forni et al. (2013). Yet glass geochemical investigations of these proximal units are still required. For the moment the cryptotephra M25/4-12-44cm provides evidence for yet another ash dispersal from the island of Lipari and further

emphasises the importance of distal archives for cataloguing eruptive events at the volcanic source.

6.4.2.4 Monte Pilato and Lami successions - distal correlations

The historical Monte Pilato tephra (776 AD) is reported as a widespread marker bed within the volcanostratigraphy of the Aeolian Islands (Lucchi et al., 2008, 2013b) and the surrounding marine records including the sediments of the Tyrrhenian (Paterne et al., 1988; Di Roberto et al., 2008; Albert et al., 2012) and Ionian (Caron et al., 2012) Seas. As mentioned above, the Lami eruptive succession is stratigraphically related by Forni et al. (2013) to activity that occurred after the 776 AD Monte Pilato eruption, and instead temporally associated with the younger, Rocche Rosse lava flow (1220 AD). This reconstruction is supported by our chemical data showing a compositional affinity between the Rocche Rosse lava flow and the Lami succession, consistent with the temporal evolution of the glasses erupted on the island. Thus if the chemically distinguishable Monte Pilato and Lami (Rocche Rosse) deposits record two temporally separate eruptions then this offers significant potential to assess their application as distinct marker beds and useful isochrons within the volcanostratigraphies of the Aeolian Islands.

As an example, different stratigraphic reconstructions on Vulcano suggest the presence of tephra layers associated with the last eruptions of Lipari. Particularly, a white HKCA rhyolitic tephra layer is recognized above the Palizzi deposits from La Fossa on top of the Vulcanello platform (Keller, 1980a; De Astis et al., 2013; Di Traglia et al., 2013; Fusillo et al., 2015), but is attributed to differing proximal units on Lipari. In fact, this tephra layer is attributed to either the 776 AD Monte Pilato (Keller, 1980a; De Astis et al., 2013) or the 1220 AD Rocche Rosse eruptions (Di Traglia et al., 2013; Fusillo et al., 2015). No unequivocal chronological information comes out from the age of the underlying deposits, considering that there are contrasting ages for the Vulcanello platform of 1.9 ka by Voltaggio et al. (1995) or 1000–1230 AD by Arrighi et al. (2006). However, if accepted, the latter age would exclude the

occurrence of a Monte Pilato tephra on Vulcanello, instead indicating a likely correlation with the Rocche Rosse or Lami eruptions. A future comparison of glass compositions from this tephra with our proximal dataset could provide important insight regarding this issue.

Distally, the tephra TIR2000-IV-7cm reported from the Marsili Basin, southern Tyrrhenian Sea, was previously correlated with the Monte Pilato eruption (Di Roberto et al., 2008; Albert et al., 2012). However, it shows major element glass compositions that are more consistent with the Lami succession, although there is partial overlap those of the Monte Pilato **(Fig. 10b).** At a trace element level both the higher and lower LREE concentrations distinctive of the Monte Pilato and Lami successions are observed in the distal tephra (**Fig. 10c-d**). Thus it would seem that the tephra TIR2000-IV-7cm contains glass shards related to both Monte Pilato and Lami successions. This tephra is interpreted as a monogenetic turbidite (Di Roberto et al., 2008; Albert et al., 2012), which could be related to PDC input or collapse contemporaneous or subsequent to the Lami eruptive activity, thus possibly incorporating older Monte Pilato products.

In the northern Ionian Sea sediments a cryptotephra layer is reported by Caron et al. (2012) in core MD90-918 spanning 2-5 cm and dated at ca. 0.6 cal ka BP (1321-1349 AD). Our major element proximal glass data might support a better correlation of this cryptotephra with the Lami succession rather than the Monte Pilato which is consistent with the age of the distal tephra. Trace element analysis of this distal layer would help verify its precise proximal associations on Lipari.

6.4.3 Salina

6.4.3.1 Upper Pollara – distal correlations (E-2)

Currently the only distal occurrence of a Salina-derived tephra is with the E-2 layer in the marine core KET8003 from the southern Tyrrhenian Sea reported by Paterne et al. 1988. Our proximal glass dataset supports the correlation of this tephra layer with the Upper Pollara eruption. Glass data from Paterne et al. (1988) show that the E-2 tephra presents a

HKCA rhyolitic affinity with higher CaO at overlapping FeOt compared to the Lipari glasses, which is indeed consistent with our proximal data for the Upper Pollara glasses **(Fig. 7b)**. Compared to the stratigraphically variable compositions of the proximal Upper Pollara glasses, high K_2O, and lower CaO and FeO values might indicate that the E-2 layer has a closest affinity to the glasses erupted midway through the eruption, corresponding to ERU3 and ERU4 deposits. New glass data for the E-2 tephra is required to more reliably test such an eruptive unit specific correlation.

6.5 Towards an integrated proximal-distal event stratigraphy: insights from past Aeolian Island ash dispersals and the associated volcanic processes

Proximal glass data presented here coupled with stratigraphic and chronological information from the literature has helped verify some proximal-distal tephra correlations, which is crucial for the future application of Aeolian island tephra deposits as isochronous markers. Some distal marine tephra layers from the Aeolian Islands cannot be attributed to precise proximal equivalents, but the proximal data presented here allows the distal layers to be assigned to a specific source volcano. The lack of proximal equivalents for some distal layers testifies to the sometimes incomplete nature of volcanic island stratigraphies, typically due to limited onland exposure and/or erosion of deposits (e.g., Brown and Branney, 2013; Cassidy et al., 2014; Tomlinson et al., 2014). This also emphasises the importance of detailed proximal sampling strategies that have been employed at other volcanic centres (e.g., Campi Flegrei; Smith et al., 2011). Linking these distal layers to volcanic source using glass chemistry is crucial to better reconstructing the eruptive history of volcanic centres. Through robust geochemical characterisation and correlation, these distal records help constrain the tempo and frequency of volcanism at individual centres (e.g., Wulf et al., 2004; Smith et al., 2011; Tomlinson et al., 2012; Albert et al., 2013; Fontijn et al., 2014; Tomlinson et al., 2014), which is essential for future hazard assessments (e.g., Sulpizio et al., 2014). The proximal-distal tephra correlations presented in this study are the first step towards the construction of a composite eruptive event stratigraphy for the Aeolian Islands during the last 50 ka (**Fig. 11**).

Lipari and Vulcano have been the most active islands in the last 50 ka and are the sources of some widespread ash layers. There are at least six HKCA explosive eruptions from Lipari (Fig. 11), which include the Monte Guardia (24,650-27,100 cal yrs BP) and Vallone del Gabellotto (8,430-8,730 cal yrs BP) units that are important stratigraphic and chronological markers in the Aeolian Islands. The Vallone del Gabellotto/E-1 and the E-11 marine tephra layers are the most widespread ash dispersals from the islands and enable the synchronisation of cores from the Tyrrhenian, Ionian and Adriatic Seas (Fig. 11). However, the proximal equivalents of the E-11, and two other Lipari-derived distal tephra layers (M25/4-12-44cm and MD90-918-820cm), have not yet been identified proximally. At least six ash dispersals, recorded in central Mediterranean marine cores, have been confidently assigned to explosive activity occurring on Vulcano. Whilst the occurrence of the Quadara pumices on Capo Milazzo, Sicily, indicates that the eruption plume of this sub-Plinian eruption extended south. Other precise proximal-distal correlations to specific Vulcano eruptions have not been possible, this is possibly related to the sampling strategy that was restricted to an extent by the lack of outcrops, but could also reflects the paucity of directly comparable published glass data from the distal marine cores owing to the use of different analytical conditions. The compositional differences between the proximal Vulcano units are subtle, so correlating distal layers to particular eruption deposits is challenging and requires precise data. Tephra units erupted from Salina and Stromboli are not prevalent in the distal records, suggesting the lower frequency of explosive phases capable of widespread ash dispersal.

Some of the largest eruptions on the Aeolian Islands in the last 50 ka, with thick sub-Plinian fallout deposits (e.g., Lower Pollara), are not observed in the distal records of the Central Mediterranean Sea. These explosive eruptions are typically estimated to have ejected material high into the atmosphere (7-14 km; e.g., Calanchi et al., 1993; Biass et al., 2016), yet the distribution of these deposits is seemingly restricted to proximal and medial areas, on the neighbouring islands, up to 15-20 km form vent (e.g., Lower Pollara on Lipari and

Quadrara on Capo Milazzo). The dominant westerlies in the region might restrict northward dispersal of Aeolian Island tephras, and one possibility is that the absence of certain tephra units from the southern Tyrrhenian Sea records, may reflect highly variable sedimentation rates (e.g., Paterne et al., 1986; Morabito et al., 2014), and stratigraphic gaps possibly caused by active canyons and tectonics in the basin.

Our volcanic glass chemistry and integrated proximal-distal event stratigraphy indicates that the tephra layers that are most widely dispersed are from eruptions that produced PDCs (e.g., Vallone del Gabellotto, Upper Pollara). The Monte Guardia sub-Plinian eruption is characterised by both fall (purely magmatic) and PDC deposits, in which the latter stages are related to magma-water interaction (e.g., Forni et al., 2013). The glass compositions of the Monte Guardia opening fall deposits are heterogeneous, and are seemingly restricted to Lipari Island. The medial PDC deposits at Gelso, southern Vulcano (Lucchi et al., 2010; 2013b), are exclusively comprised of the most evolved, high-SiO_2 rhyolitic glasses, which are consistent with those found in the distal Lago di Pergusa, Sicily, indicating that the PDC phase is the most widely dispersed, and provides evidence for a dominant long-distance SW ash dispersals (**Fig. 1a**). This finding is consistent with the study by Smith et al. (2016) that shows that the most far-travelled component of large Campanian Ignimbrite eruption is associated with the co-PDC plume rather than the Plinian phase.

Mafic glass compositions with a Vulcano-derived chemical affinity are found up to 400 km from source in Ionian and Adriatic marine records. The lack of prominent, thick proximal eruptive units, corresponding to these distal tephra layers indicates that the eruptions were most likely smaller explosive events. Since these tephra are more widely dispersed than some of the more prominent, larger, eruptions on the islands it implies that the particles were finer and fragmentation was very efficient. Water-magma interaction was probably a necessary mechanism for generating such fine-grained material (e.g., Self and Sparks, 1978). The interaction of more basic magmas and water during modest size eruption has the potential to generated and widely disperse fine-grained material as testified by the 2010

Eyjafjallajökull plume that extended from Iceland and across Europe (Gudmundsson et al., 2012). On Vulcano itself, evidence for hydromagamatic activity within the La Fossa caldera is recognised in the form of the massive to laminated ash beds of the Upper Tufi di Grotte dei Rossi outcropping in the Piano area of Vulcano (e.g., Dellino et al., 2011), this eruptive scenario might be considered as an analogue for the type of activity responsible for producing distal Vulcano-derived mafic ash layers so far from source. Furthermore, the presence of Lipari-derived tephra in the distal records without known, prominent eruptive units, on the island, could lend further support to the hypothesis that smaller eruptions with effective ash fragmentation processes are capable of dispersing material over significant distances (up to 400 km). This has important hazard implications as many volcanic hazard evaluations are based on the largest eruptions, and don't always take into account the potential disruption from these small volcanic eruptions that may interact with water.

7. Conclusions

Proximal deposits of some of the most widely recognised explosive eruptions on the Aeolian Islands during the last 50 ka have been subjected to detailed sampling and geochemical characterisation (EMPA and LA-ICP-MS) to provide a comprehensive database of glass compositions (>1000 analyses) for the purpose of evaluating proximal-distal tephra correlations. This dataset has enabled the establishment of an integrated proximal-distal explosive event stratigraphy for the Aeolian Islands, and also facilitates distal-distal tephra correlations between central Mediterranean sedimentary archives. The geochemical investigations demonstrate that;

(1) The tephra deposits erupted from the different Aeolian Islands are mostly geochemically diverse with glasses ranging from CA through to KS in composition.

(2) Some individual eruptions show diagnostic geochemical heterogeneity, some in the form of chemo-stratigraphic variations, whilst others spatially.

(3) Vulcano and Stromboli have erupted some KS and SHO eruptive products with broadly overlapping compositions, however these can easily be separated using either their TiO_2 contents at a given SiO_2 concentration or their HFSE/Th ratios.

(4) On Lipari successive eruptive units have HKCA rhyolitic major and minor element glass compositions that are largely indistinguishable through time, crucially however, temporal changes in the LREE and Th concentration of these volcanic glasses able the units to be distinguished. This is a useful demonstration of trace element glass analysis greatly enhancing the potential to discriminate different eruptive units from a single volcanic centre.

(5) New distal occurrences of Lipari derived tephra layers are recognised in the southern Ionian Sea (M25/4-12), one extending south-ward extend to the Vallone del Gabellotto tephra.

(6) The integrated proximal-distal event stratigraphy suggests that the most widely dispersed Aeolian Island tephra deposits are likely to relate to PDCs.

Acknowledgements

References

Albert, P.G., Tomlinson, E.L., Smith, V.C., Di Roberto, A., Todman, A., Rosi, M., Marani, M., Muller, W., Menzies, M.A., 2012. Marine-continental tephra correlations: Volcanic glass geochemistry from the Marsili Basin and the Aeolian Islands, Southern Tyrrhenian Sea, Italy. Journal of Volcanology and Geothermal Research, 229-230, 74-94

Albert, P.G., Tomlinson, E.L., Lane, C.S., Wulf., S., Smith, V.C., Coltelli, M., Keller, J., Lo Castro, D., Manning, C.J., Muller, W., Menzies, M.A., 2013. Late glacial explosive activity on

Mount Etna: implications for proximal-distal tephra correlations and the synchronisation of Mediterranean archives. Journal of Volcanology and Geothermal Research 265, 9-26.

Albert, P.G., Hardiman, M., Keller, J, Tomlinson, E.L., Bourne, A, J., Smith, V.C. Wulf, S., Zanchetta, G., Sulpizio, R., Müller, U.C., Pross, J., Ottolini, L., Matthews, I.P., Blockley, S.P., Menzies, M.A., 2015. The Y-3 tephrostratigraphic marker revisited: new diagnostic glass geochemistry, improved chronology and climatostratigraphic interpretations. Quaternary Science Reviews, 118, 105-121.

Albert, P.G., 2012. Volcanic glass chemistry of Italian proximal deposits link to distal archives in the central Mediterranean region. PhD Thesis, Royal Holloway University of London.

Allan, A.S.R., Baker, J.A., Carter, L., Wysoczanksi, R.J., 2008. Reconstructing the Quaternary evolution of the world's most active silicic volcanic system: insights from a similar to 1.65 Ma deep ocean tephra record sourced from Taupo Volcanic Zone, New Zealand. Quaternary Science Reviews 27 (25–26), 2341–2360.

Arrighi, S., Tanguy, J.C., Rosi., M. 2006. Eruptions of the last 2200 years at Vulcano and Vulcanello (Aeolian Islands, Italy) dated by high-accuracy archeomagnetism. Phys Earth Planet Inter 159 (3-4): 225-233.

Barberi, F., Gasparini, P., Innocenti, F., Villari, L., 1973. Volcanism of the Southern Tyrrhenian Sea and its geodynamic implications. J Geophys Res 78: 5221-5232.

Bertagnini, A., Landi, P., 1996. The Secche di Lazzaro pyroclastics of Stromboli volcano: a phreatomagmatic eruption related to the Sciara del Fuoco sector collapse. Bulletin of Volcanology, 58, 239-245.

Beccaluva, L., Gabbianelli, G., Lucchini, F., Rossi, P.L., Savelli, C., 1985. Petrology and K/Ar ages of volcanics dredged from the Aeolian Seamounts: implications for geodynamic evolution of the southern Tyrrhenian basin. Earth Plan Sci Lett 74:187-208.

Biass, S., Bonadonna, C., di Traglia, F., Pistolesi, M., Rosi, M., Lestuzzi, P., 2016. Probabilistic evaluation of the physical impacts of future tephra fallout events for the Island of Vulcano, Italy. Bull Volcanol 78:37 DOI 10.1007/s00445-016-1028-1

Bigazzi, G., Coltelli, M., Norelli, P., 2003. Nuove eta delle ossidiane di Lipari determinate con il metodo delle trace di fissione. GEOITALIA 2003; Federazione Italiana di Scienze della Terra, 444-446.

Blockley, S.P.E., Pyne-O'Donell, S.D.F., Lowe, J.J., Matthews, I.P., Stone, A., Pollard, A.M., Turney, C.S.M., Molyneux, E.G. 2005. A new and less destructive laboratory procedure for the physical separation of distal glass tephra shards from sediments. Quaternary Science Reviews, 224, 16-17, 1952-1960.

Bourne, A., Lowe. J.J., Trincardi, F., Asioli, A., Blockley, S.P.E, Wulf, S., Matthews, I.P., Piva. A., Vigliotti, L., 2010. Distal tephra record for the last 105, 000 years from the core PRAD 1-2 in the Adriatic Sea: implications for marine tephrostratigraphy. Quaternary Science Reviews 29, 23-24, 1-16.

Bourne, A.J., Albert, P.G., Matthews, I.P., Wulf, S., Lowe, J.J., Asioli, A., Blockley, S.P.E., Trincardi, F. (2015). Tephrochronology of core PRAD1-2 from the Adriatic Sea: insights into Italian explosive volcanism for the period 200-80 . Quat. Sci. Rev., 116, 28-43.

Brown, R.J., Branney, M.J. 2004. Event-stratigraphy of a caldera-forming ignimbrite eruption on Tenerife: the 273ka Poris Formation. Bull. Volcanol 66, 392-416.

Capaccioni, B., Coniglio, S., 1995. Varicolored and vesiculated tuffs from La Fossa volcano, Vulcano Island (Aeolian Archipelago, Italy): evidence of syndepositional alteration processes. Bulletin of Volcanology, 57, 61-70.

Cassidy, M., Watt, S.F.L., Palmer, M.R., Trofimovs, J., Symons, W., Maclachlan, S.E., Stinton, A., 2014. Construction of volcanic records from marine sediment cores: a review and case study (Montserrat, West Indies). Earth-Science Reviews, 138, 137-155.

Calanchi, N., De Rosa, R., Mazzuoli, R., Rossi, P.L., Santacroce, R., Ventura, G., 1993. Silicic magma entering a basaltic magma chamber: eruptive dynamics and magma mixing — an example from Salina (Aeolian Islands, southern Tyrrhenian Sea). Bulletin of Volcanology 55, 504–522.

Caron, B., Siani, G., Sulpizio, R., Zanchetta, G., Paterne, M., Santacroce, R., Tema, E., Zanella, E. 2012. Late Pleistocene to Holocene tephrostratigraphic record from the Northern Ionian Sea. Marine Geology, 311-314. 41-51.

Chiarabba, C., De Gori, P., Speranza, F., 2008. The southern Tyrrhenian subduction zone: Deep geometry, magmatism and Plio-Pleistocene evolution.

Clift, P., Blusztajn, J., 1999. The trace-element characteristics of Aegean and Aeolian volcanics arc marine tephra. Journal of Volcanology and Geothermal Research 92, 321-374.

Cortes, J.A., Wilson, M., Condliffe, E., Francalanci, L., Chertkoff, D.G., 2005. The evolution of the magmatic system of Stromboli volcano during the Vancori period (26-13.8 ky). Journal of Volcanology and Geothermal Research 147, 1-2, 1-38.

Crisci, G.M., De Rosa, R., Esperanca, S., Mazzuoli, R., Sonnino, M. 1981.Temporal evolution of a three component system: The island of Lipari (Aeolian Arc, southern Italy). Bulletin of Volcanology 53. 207-221.

Crisci, G.M., Delibrias, G., De Rosa, R., Mazzuoli, R., Sheridan, M.F., 1983. Age and petrology of the Late-Pleistocene brown tuffs on Lipari, Italy. Bulletin of Volcanology 46, 241-391.

Davì, M., De Rosa, R., Donato, P., Sulpizio, R., 2011. Lami pyroclastic succession (Lipari, Aeolian Islands): A clue for unraveling the eruptive dynamics of the Monte Pilato rhyolitic pumice cone. Journal of Volcanology and Geothermal Research 201, 285-300.

Davies, S.M., Wohlfarth, B., Wastegard, S., 2004. Were there two Borrobol Tephras during the early Lateglacial period: implications for tephrochronology. Quaternary Science Reviews 23 (5-6), 581-589.

De Astis, G., Dellino, P., De Rosa, R., La Volpe, L., 1997a. Eruptive emplacement mechanism of fine grained pyroclastic deposits widespread on Vulcano Island. Bulletin of Volcanology 59, 87-102.

De Astis, G., La Volpe, L., Peccerillo, A., Civetta, L. 1997b. Volcanological and petrological evolution of Vulcano Island (Aeolian Arc, southern Tyrrhenian Sea). Journal of Geophysical Research, 102, 8021–8050.

De Astis, G., Ventura, G., Vilardo, G., 2003. Geodynamic significance of the Aeolian volcanism (Southern Tyrrhenian Sea, Italy) in light of structural, seismological, and geochemical data. Tectonics 22 (4) 1-17

De Astis, G., Lucchi, F., Dellino, P., La Volpe, L., Tranne, C. A., Frezzotti, M. L., Peccerillo, A. 2013a. Geology, volcanic history and petrology of Vulcano (central Aeolian archipelago). In: Lucchi, F., Peccerillo, A., Keller, J., Tranne, C. A. & Rossi, P. L. (eds) The Aeolian Islands Volcanoes. Geological Society, London, Memoirs, 37, 281–348.

De Astis,G.,Dellino, P.,LaVolpe, L.,Lucchi,F., Tranne,C.A. 2013b. Geological map of the island of Vulcano, scale 1:10,000 (Aeolian archipelago). In: Lucchi, F., Peccerillo, A., Keller, J., Tranne, C. A. & Rossi, P. L. (eds) The Aeolian Islands Volcanoes. Geological Society, London, Memoirs, 37, enclosed DVD.

Dellino, P., De Astis, G., La Volpe, L., Mele, D. and Sulpizio, R., 2011. Quantitative hazard assessment of phreatomagmatic eruptions at Vulcano (Aeolian Islands, Southern Italy), as obtained by combining stratigraphy, event statistics and physical modelling. Journal of Volcanology and Geothermal Research 201, 264-384.

Di Traglia, F., Pistolesi, M., Rosi, M., Bonadonna, C., Fusillo, R., Roverato, M., 2013. Growth and erosion: The volcanic geology and morphological evolution of La Fossa (Island of Vulcano, Southern Italy) in the last 1000 years. Geomorphology 194, 94-107.

Di Traglia, F., 2011. The last 1000 years of eruptive history at the La Fossa cone (Island of Vulcano, Southern Italy). PhD thesis.

De Rita, D., Dolfi, D., Cimarelli, C. 2008. Occurrence of Somma-Vesuvius fine ashes in the tephrostratigraphy record of Panarea, Aeolian Islands. Journal of Volcanology and Geothermal Research 177 (1), 197-207.

De Rosa, R., Frazzetta, G., La Volpe, L., Mazzuoli, R. 1988. The Spiaggia Lunga scoriae deposits: an example of fissural type eruption at Vulcano, Aeolian Islands, Italy. Rendiconti della Societa` Italiana di Mineralogia e Petrologia, 43, 1059–1068.

De Rosa, R., Guillou, H., Mazzuoli, R., ventura, G., 2003a. New unspiked K-Ar ages of volcanic rocks of the central and western sectors of the Aeolian Islands: Reconstruction of the volvanic stages. Journal of Volcanology and Geothermal Research 120, 161-178

De Rosa, R., Donato., Gioncada. A., Masetti, M., and Sactacroe, R., 2003b. The Monte Guardia eruption (Lipari, Aeolian Islands): an example of a reversely zoned magma mixing sequence. Bulletin of Volcanology 65, 530-543.

De Vivo, B., Rolandi, G., Gans, P.B., Calvert, A., Bohrson, W.A., Spera, F.J., Belkin, H.E. 2001. New constraints on the pyroclastic eruptive history of the Campanian volcanic plain (Italy). Mineralogy and Petrology, 73: 47-65.

Di Roberto, A., Rosi, M., Bertagnini, A., Marani, M.P., Gamberi, F., Del Principe, A., 2008. Deep water gravity core from the Marsili Basin (Tyrrhenian Sea) records Pleistocene-Holocenic explosive events and instabilities of the Aeolian Island Archipelago, (Italy). Journal of Volcanology and Geothermal Research 177 (1), 133-144.

Di Traglia, F., 2011. "The last 1000 years of eruptive activity at the Fossa Cone (Island of Vulcano, Southern Italy)", PhD Thesis, University of Pisa, Italy, unpublished thesis.

Ellam, R.M., Menzies, M.A., Hawkesworth, C.J., Leeman, W.P., Rosi, M., and Serri, G., 1988. The transition from calc-alkaline to potassic orogenic magmatism in the Aeolian Islands, Southern Italy. Bulletin of Volcanology 50. 387-398.

Ellam, R.M., Hawkesworth, C.J., Menzies, M.A., Rogers, N.W., 1989. The volcanism of southern Italy: role of subduction and relationship between potassic and sodic alkaline magmatism. J Geophys Res. 94: 4589-4601.

Fontijn, K., Lachowycz, S.M., Rawson, H., Pyle, D.M., Mather, T.A., Maranjo, J.A., Moreno-Roa, H., 2014. Late Quaternary tephrostratigraphy of southern Chile and Argentina. Quaternary Science Reviews, 89, 70-84.

Forni, F., Lucchi, F., Peccerillo, A., Tranne, C.A., Rossi, P.L., Frezzotti, M.L. 2013. Stratigraphic and geological evolution of the Lipari volcanic complex (central Aeolian archipelago). In Lucchi, F., Peccerillo, A, Keller, J., Tranne, C.A., Rossi, P.L., (eds) 2013. The Aeolian islands Volcanoes. Geological society, London, Memoirs, 37, 213-279.

Francalanci, L., Taylor, S.R., McCulloch, M.T., Woodhead, J.D., 1993. Geochemical and isotopic variations in the calc-alkaline rocks of Aeolian arc, southern Tyrrhenian Sea, Italy: constraints on magma genesis. Contributions to Mineralogy Petrology 113, 300–313.

Francalanci, L., Lucchi, F., Keller, J., De Astis G., Tranne, C.A., 2013. Eruptive, volcano-tectonic and magmatic history of the Stromboli volcano (north-eastern Aeolian archipelago). In: Lucchi, F., Peccerillo, A., Keller, J., Tranne, C. A. & Rossi, P. L. (eds) The Aeolian Islands Volcanoes. Geological Society, London, Memoirs, 37, 397-471.

Frazzetta, G., La Volpe, L., & Sheridan, M. F. (1983). Evolution of the Fossa cone, Vulcano. Journal of Volcanology and Geothermal Research, 17(1), 329-360.

Frazzetta, G., Gillot, P. Y., La Volpe, L., & Sheridan, M. F. (1984). Volcanic hazards at Fossa of Vulcano: data from the last 6,000 years. Bulletin volcanologique, 47(1), 105-124.

Fusillo, R., Di Traglia, F., Gioncada, A., Pistolesi, M., Wallace, P.J., Rosi, M., 2015. Deciphering post-caldera volcanism: insight into the Vulcanello (Island of Vulcano, Southern Italy) eruptive activity based on geological and petrological constraints. Bull Volcanol 77:76. DOI 10.1007/s00445-015-0963-6

Gertisser, R. Keller, J. 2000. From basalt to dacite: origin and evolution of the calc-alkaline series of Salina, Aeolian Arc, Italy. Contributions to Mineralogy and Petrology. 139 (5), 607-626.

Gioncada, A., Mazzuoli, R., Bisson, M., Pareschi, M.T., 2003 Petrology of volcanic products younger than 42 ka on the Lipari-Vulcano complex (Aeolian Islands, Italy): an example of volcanism controlled by tectonics. Journal of Volcanology and Geothermal Research 122, 191–220.

Giordano, G., Porreca, M., Musacchio, P. and Mattei., 2008. The Holocene Secche di Lazzaro phreatomagmatic succession (Stromboli, Italy): evidence of pyroclastic density current origin deduced by facies analysis and AMS flow directions. Bulletin of Volcanology 70, 1221-1236.

Gudmundsson, M., Thordarson, T., Höskuldsson, A., Larsen, G., Björnsson, H., Prata, F.J., Oddsson, B., Magnússon, E., Högnadóttir, T., Petersen, G.N., Hayward, C.L., Stevenson, J.A., Jónsdóttir, I., 2012. Ash generation and distribution from the April-May 2010 eruption of Eyjafjallajökull, Iceland. Scientific Reports, 2, 572.

Gurioli L., Sbrana A., 1999. Caratterizzazione stratigrafica e sedimentologica dei depositi della eruzione della Breccia di Commenda(Isola di Vulcano), Atti Societa Toscana Scienze Naturali, 106, 13-25.

Gvirtzman, Z., Nur, A., 1999. The formation of Mount Etna as the consequence of slab roll back. Nature, 401. 782-785.

Insinga, D.D., Tamburrino, S., Lirer, F., Vezzoli, L., Barra, M., De Lange, G.J., Tiepolo, M., Vallefuoco, M., Mazzola, S., Sprovieri, M. 2014. Tephrochronology of the astronomically-tuned KC01B deep-sea core, Ionian Sea: insights into the explosive activity of the Central Mediteranean area during the last 200 ka. Quaternary Science Review, 85, 63-84.

Jochum, K.P. et al., 2006. MPI-DING reference glasses for in situ microanalysis: 581 New reference values for element concentrations and isotope ratios. 582 Geochemistry Geophysics Geosystems. 7, (2).

Keller, J., 1980. The island of Salina. Rendiconti della Società Italiana di Mineralogia e Petrologia. 36, pp 489–524.

Keller, J., Kraml, M., Scheld, A., 1996. Late Quaternary tephrochronological correlation between deep-sea sediments and the land record in the Central Mediterranean. In 30th International Geological Congress, Beijing, vol 3, pp 204.

Keller, J., 2002. Lipari's Fiery Past: Dating the Medieval Pumice Eruption of Monte Pelato, Internat. Conference UNESCO-Reg Siciliana, Lipari, September 29–October 2

Keller, J., Ryan, W.B.F., Ninkovich, D., Altherr, R., 1978. Explosive volcanic activity in the Mediterranean over the past 200,000 yr as recorded in deep-sea sediments. Geological Society of America Bulletin 89, 591–604.

Lane, C.S., Cullen, V.L., White, D., Bramham-Law, C.W.F., Smith, V.C. 2014. Cryptotephra as a dating and correlation tool in archaeology. Journal of Archaeological Science, 42, 42-50.

Lucchi, F., 2009. Late-Quaternary marine terrace deposits as tools for wide-scale correlation of unconformity-bounded units in the volcanic Aeolian archipelago (southern Italy). Sedimentary Geology, 216, 158–178.

Lucchi, F., Tranne, C.A., Calanchi, N., Rossi, P.L., Keller, J. 2007. The stratigraphic role of marine deposits in the geological evolution of the Panarea volcano (Aeolian Islands, Italy). Journal of the Geological society of London, Vol 164, pp 983-996.

Lucchi, F., Tranne, C.A., De Astis, G, Keller, J., Losito, R., Morche, W., 2008. Stratigraphy and significance of Brown Tuffs on the Aeolian Islands (southern Italy). Journal of Volcanology and Geothermal Research 177, 49–70.

Lucchi, F., Tranne, C.A., Rossi, P.L., 2010. Stratigraphic approach to geological mapping of the Late Quaternary island of Lipari (Aeolian archipelago, Southern Italy). In Groppelli, G., Viereck-Grotte, L., 2010. Stratigraphy and Geology of Volcanic Areas. The Geological society of America. Special Paper 464.

Lucchi, F., Gertisser, R., Keller, J., Forni, F., De Astis, G., Tranne, C. A. 2013a. Eruptive history and magmatic evolution of the island of Salina (central Aeolian archipelago). In: Lucchi, F., Peccerillo, A., Keller, J., Tranne, C. A. & Rossi, P. L. (eds) The Aeolian Islands Volcanoes. Geological Society, London, Memoirs, 37, 155–211

Lucchi, F., Keller, J., Tranne, C., 2013b. Regional stratigraphic correlations across the Aeolian archipelago (southern Italy). In: Lucchi, F., Peccerillo, A., Keller, J., Tranne, C. A. & Rossi, P. L. (eds) The Aeolian Islands Volcanoes. Geological Society, London, Memoirs, 37, 55–81. doi: 10.1144/M37.6

Lucchi, F., Tranne, C. A., Forni, F., Rossi, P. L. 2013b2013c. Geological map of the island of Lipari, scale 1:10 000 (Aeolian archipelago). In: Lucchi, F., Peccerillo, A., Keller, J., Tranne, C. A. & Rossi, P. L. (eds) The Aeolian Islands Volcanoes. Geological Society, London, Memoirs, 37, enclosed DVD.

Lucchi, F., Tranne, C. A., Peccerillo, A., Keller, J., Rossi, P. L. 2013d. Geological history of the Panarea volcanic group (eastern Aeolian archipelago). In: Lucchi, F., Peccerillo, A., Keller, J., Tranne, C. A. & Rossi, P. L. (eds) The Aeolian Islands Volcanoes. Geological Society, London, Memoirs 37, 349–393.

Mandarano, M., Paonita, A., Martelli, M., Viccaro, M., Nicotra, E., & Millar, I. L., 2016. Revealing magma degassing below closed-conduit active volcanoes: Geochemical features

of volcanic rocks versus fumarolic fluids at Vulcano (Aeolian Islands, Italy). *Lithos,* 248–251, 272–287.

Matthews, I.P., Trincardi, F., Lowe, J.J., Bourne, A.J., MacLeod, A., Abbott, P.M., Anderson, N., Asioli, A., Blockley, S.P.E., Lane, C.S., Oh, Y.A., Satow, C.S., Staff, R.A., Wulf, S. 2015. Developing a robust tephrochronological framework for Late Quaternary marine records in the Southern Adriatic Sea: new data from core station SA03-11. Quaternary Science Reviews, 118, 84-104.

Morche, W., 1988. Tephrochronologie der Aolischen Inseln. Unpublished PhD Thesis, Albert-Ludwigs-Universitat Freiburg, Germany.

Morabito, S Petrosino, P., Milia, A., Sprovieri, M., Tamburrino, S., 2014. A multidisciplinary approach for reconstructing the stratigraphic framework of the last 40 ka in a bathial area of the eastern Tyrrhenian SeaGlob. Planet. Chang., 123 (2014), pp. 121–138

Narcisi, B., 2002. Tephrostratigraphy of the Late Quaternary lacustrine sediments of Lago di Pergusa (central Sicily). Bollenttino della Societa geologica italiana. 12 (2), 211-219.

Negri, A., Capotondi, L., Keller, J., 1999. Calcareous nannofossils, planktonic foraminifera and oxygen isotopes in the Late Quaternary Sapropels of the Ionian Sea. Marine Geology 157. 89-103.

Paterne, M., Guichard, F., Labeyrie, J., Gillot, P. Y. & Duplessy, J. C. 1986. Tyrrhenian Sea tephrochronology of the oxygen isotope record for the past 60,000 years. Marine Geology 72, 259-285.

Paterne, M., Guichard, F., Labeyrie, J. 1988. Explosive activity of the South Italian volcanoes during the past 80,000 years as determined by marine tephrochronology. Journal of Volcanology and Geothermal Research 34, 153–172.

Peccerillo, A., De Astis, G., Faraone, D., Forni, F., Frezzotti, M. L. 2013. Compositional variation of magmas in the Aeolian arc: implications for petrogenesis and geodynamics. In: Lucchi, F., Peccerillo, A., Keller, J., Tranne, C. A. & Rossi, P. L. (eds) The Aeolian Islands Volcanoes. Geological Society, London, Memoirs, this volume, 489–508.

Petrone, C.M., Braschi, E., Francalanci, L., 2009. Understanding the collapse–eruption link at Stromboli, Italy: A microanalytical study on the products of the recent Secche di Lazzaro phreatomagmatic activity. Journal of Volcanology and Geothermal Research 188 (4), 315-332.

Piochi, M., De Astis, G., Petrelli, M., Ventura, G., Sulpizio, R., Zanetti, A., 2009. Constraining the recent plumbing system of Vulcano (Aeolian Arc, Italy) by textural, petrological, and fractal analysis: The 1739 AD Pietre Cotte lava flow. Geophys. Geosy., 10, doi:10.1029/2008GC002176

Porreca, M., Giordano, G., Mattei, M., Musacchio, P. 2006. Evidence of two Holocene phreatogmagmatic eruptions at Stromboli volcano (Aeolian Islands) from paleomagnetic data. Geophysical Research Letters, Vol 33.

Reimer, P.J., Bard, E., Bayliss, A., Beck, J.W., Blackwell, P.G., Bronk Ramsey, C., Buck, C.E., Edwards, R.L., Friedrich, M., Grootes, P.M., Guilderson, T.P., Haflidason, H., Hajdas, I., Hatté, C., Heaton, T.J., Hoffmann, D.L., Hogg, A.G., Hughen, K.A., Kaiser, K.F., Kromer, B., Manning, S.W., Niu, M., Reimer, R.W., Richards, D.A., Scott, E.M., Southon, J.R., Staff, R.A., Turney, C.S.M. and van der Plicht, J. (2013) "IntCal13 and Marine13 radiocarbon age calibration curves 0-50,000 years cal BP". _Radiocarbon 55 (4), 1869-1887_

Rosi, M., Bertagnini, A., Landi, P., 2000. Onset of the persistent activity at Stromboli Volcano (Italy). Bulletin of Volcanology 62 (4–5), 294–300.

Rosi, M., Pistolesi, M., Bertagnini, A., Landi, P., Pompilio, M., Di Roberto, A. 2013. Stromboli Volcano, Aeolian Islands (Italy): present eruptive activity and hazards. In: Lucchi, F., Peccerillo, A., Keller, J., Tranne, C. A. & Rossi, P. L. (eds) The Aeolian Islands Volcanoes. Geological Society, London, Memoirs, 37, 471–488.

Self, S., Sparks, R. S. J., 1978. Characteristics of widespread pyroclastic deposits formed by the interaction of silicic magma and water. Bulletin Volcanologique, 41(3), 196 doi.org/10.1007/BF02597223

Siani, G., Sulpizio, R., Paterne, M., Sbrana, A., 2004. Tephrostratigraphy study for the last 18,000 14C years in a deep-sea sediment sequence for the South Adriatic. Quaternary Science Reviews 23, 2485–2500.

Smith, V.C., Isaia, R., & Pearce, N.J.G., 2011. Tephrostratigraphy of post-15 kyr Campi Flegrei eruptions: implications for eruption history and chronostratigraphic markers. Quaternary Science Reviews 30 (25-26), 3638-3660.

Smith, V.C., Isaia, R., Engwell, S., Albert, P.G., Tephra dispersal during the Campanian Ignimbrite (Italy) eruption: implications for ultra-distal ash transport during the large caldera-forming eruption. Bulletin of Volcanology, 78:45 DOI: 10.1007/s00445-016-1037-0

Soligo, M., De Astis, G., Delitala, M.C., La Volpe, L., Tadderucci, A., Tuccimei, P., 2000. Diequilibri nella serie dell uranio nei prodotti dell isola di Vulcano: cronologia isotopica e implixazioni magmatologiche. 2 Forum Italiano di Scienze della Terra Riassunti, Plinus. 22, 347-349.

Speranza, F., Pompolio, M., D'Ajello Coraccioli, F., Sagnotti, L., 2008. Holocene eruptive history of the Stromboli volcano: Constraints from paleomagnetic dating. Journal of Geophysical research, 113, B9.

Sulpizio, R., De Rosa, R., Donato, P., 2008. The influence of variable of topography on the depositional behavior of pyroclastic density currents: The examples of the Upper Pollara eruption. Journal of Volcanology and Geothermal Research 175, 367-385.

Sulpizio, R., Zanchetta, G., Caron, B., Dellino, P., Mele, D., Giaccio, B., Insinga, D., Paterne, M., Siani, G., Costa, A., Macedonio, G., Santacroce, R. 2014. Volcanic ash hazards in the Central Mediterranean assessed from geological data. Bull Volcanol 76, 866.

Sun, S., McDonough, W.F., 1989. Chemical and isotopic systematics of 630 oceanic basalts: implications for mantle composition and processes. In: 631 A.D. Saunders, Norry, M.J. (Editor), Magmatism in Ocean Basins.

Tibaldi, A., Corazzato, C., Marani, M., & Gamberi, F. (2009). Subaerial-submarine evidence of structures feeding magma to Stromboli Volcano, Italy, and relations with edifice flank failure and creep. *Tectonophysics*, *469*(1), 112-136.

Tomlinson, E.L., Thordarson, T., Muller, W., Thirlwall, M,. Menzies, M.A., 2010. Microanalysis of tephras by LA-ICP-MS- Strategies, advantages and limitations assessed using the Thorsmork ignimbrite (Southern Iceland). Chemical Geology 279, (3-4), 73-89.

Tomlinson, E., Arienzo, I., Civetta, L., Wulf, S., Smith, V.C., Hardiman, M., Lane, C.S., Carandente, A., Orsi, G., Rosi, M., Muller, W., Thirwall, M.F., Menzies, M. 2012a. Geochemistry of the Phlegraean Fields (Italy) proximal sources for major Mediterranean tephras: implications for the dispersal of Plinian and co-ignimbritic components of explosive eruptions. Geochimica et Cosmochimica Acta

Tomlinson, E.L., Kinvig, H.S., Smith, V.C., Blundy, J.D., Gottsmann, J., Muller, W., Menzies, M.A. 2012b: The Upper and Lower Nisyros Pumices: Revisions to the Mediterranean tephrostratigraphic record using micron-beam glass geochemistry. Journal of Volcanology and Geothermal Research.

Tomlinson, E.L., Albert, P.G., Wulf, S., Brown, R., Smith, V.C., Keller, J., Orsi, G., Bourne, A.J., Menzies, M.A. 2014. Age and geochemistry of tephra layers from Ischia, Italy: constraints from proximal-distal correlations with Lago Grande di Monticchio. Journal of Volcanology and Geothermal Research, 287, 22-39.

Tomlinson, E.L., Smith., V.C., Albert, P.G., Aydar, E., Civetta, L., Cioni, R., Cubukcu, E., Gertisser, R., Isaia, R., Menzies, M.A., Orsi, G., Rosi, M., Zanchetta, G, 2015. The major and trace element glass compositions of the productive Mediterranean volcanic sources: tools for correlating distal tephra layers in and around Europe. Quaternary Science Reviews, 118, 48-66.

Voltaggio, M., Branca, M., Tuccimci, P., Tecce, F. 1995. Leaching procedure used in dating young potassic volcanic rocks by the 226Ra/230Th method. Earth and Planetary Science Letters 136, 123-131.

Wulf, S., Kraml, M., Brauer, A., Keller, J., Negendank, J.F.W., 2004. Tephrochronology of the 100 ka lacustrine sediment record of Lago Grande di Monticchio (southern Italy). Quaternary International 122, 7–30.

Table and Figure captions

Table 1: Simplified volcanic history of the Aeolian Islands proximally investigated in this study. Comprehensive details on the volcanic history of Vulcano (De Astis et al. 2013; and reference therein), Lipari (Forni et al. 2013; and reference therein); Salina (Lucchi et al.,

2013a; references therein) and Stromboli (Francalanci et al., 2013; Rosi et al., 2013; and references therein) are available in the references listed. For whole-rock chemical classification abbreviations refer to the text.

Table 2: Proximally investigated and geochemically characterised tephra units explosively erupted on the Aeolian Islands during approximately the last 50 ka included in this study. Sampled pumice, scora and ash deposits sampled from each island are listed in relative stratigraphic order from youngest to oldest and sampling localities correspond with Figure 1. Literature references are given for deposits sampled following well established published stratigraphies, whilst sampling that follows our new stratigraphic investigations of the deposits are denoted by a † symbol, these interpretations builds on the referenced published findings and more detailed descriptions are provided in **Supplementary material 1**. All radiocarbon ages used have been recalibrated using the relevant IntCal13 or Marine13 calibration curves (Reimer et al., 2013) in OxCal4.2 and uncertainties are given at the 95.4% probability range. Ages presented for the Lower Pollara (Salina) and Monte Guardia (Lipari) eruptions are based on a new Bayesian age-model incorporating ^{14}C analyses of charcoal fragments form the Brown Tuff deposits immediately above and below the respective tephra units (all details, including the OxCal code, can be found in **Supplementary material 2**). References; (1) Di Traglia, 2011; (2) Di Astis et al., 2003; (3) Piochi et al., (2009); Capaccioni and Coniglio, (1995); (5) Biass et al. (2015); (6) De Astis et al., (1997a); (7) Dellino et al. (2011); (8) Gurioli and Sbrana (1999); (9) Di Traglia et al. (2013); (10) Frazzetta et al. (1984); (11) Arrighi et al. (2006); (12) Voltagio et al. (1995); (13) Albert et al. (2012); (14) Lucchi et al. (2008); De Astis et al., 2013a; (16) De Rosa et al. (2003a); (17) Morche, (1988); (18) Soligo et al. (2000); (19) Davì et al. (2012); (20) Forni et al. (2013); (21) Lucchi et al. (2013b); (22) Bigazzi et al. (2003); (23) Keller, (2002); (24) Crisci et al. (1991); (25) Lucchi et al. (2010); (26) Siani et al. (2004); (26) Crisci et al. (1981); (28) De Rosa et al. (2003b); (29) Di Rita, et al. (2008); (30) Crisci et al. (1983); (31) Lucchi et al. (2013c); (32) Sulpizio et al. (2008); (33) Lucchi et al. (2013a); (34) Keller, (1980); (35) Calanchi et al.

(1993); (36) Petrone et al. (2009); (37) Francalanci et al. (2013); (38) Speranza et al. (2008); (39) Porrecca et al. (2006).

Table 3: Representative major and minor element glass compositions of tephra units included in the study. A complete geochemical data-set is provided in **Supplementary material 3**.

Table 4: Representative trace element glass compositions of the tephra units included in this study. A complete geochemical data-set is provided in **Supplementary material 3**. Abbreviations are as follows; Tra/Trachyte; Rhy/Rhyolite; Pho-Tra/Phono-trachytic; Bas-TraA/Basaltic trachy-andesite; TraA/Trachy-andesite.

Table 5: Incompatible trace element ratios useful for fingerprinting tephra included in this study. */K-series and †/Shoshonitic.

Figure 1: DEM images of the Aeolian Islands (Southern Tyrrhenian Sea) showing the sampling locations of tephra units investigated in this study (red stars). Sample site numbers conform to **Table 2**. The insert (**a**) is a map of the central Mediterranean showing the location of key distal sedimentary archives used in this study for correlations (see text for references): (1) M25/4-12, (2) M25/4-13, (3) M25/4-11, (4) KC01-B, (5) MD90-918, (6) KET8011, (7) KET8004, (8) KET8003, (9) SA03-11, (10) MD90-917, (11) PRAD1-2, (12) Lago Grande di Monticchio, (13) Lake Ohrid, (14) Lake Prespa, (15) Lago Pergusa, (16) Capo Milazzo.

Figure 2: A selection of representative outcrop photographs of the investigated tephra units. The sample site numbers conform to **Table 2** and **Figure 1**. Descriptions of sub-divisions of individual tephra units are provided in **Supplementary material 1**. (a) Stratigraphic succession of the southern dome complex of Lipari, demonstrating the Punta del Perciato, Falcone and Monte Guardia tephra units interbedded with different Brown Tuff layers [site number 14]. (b) A closer view of the pumiceous deposits of the Punta del Perciato in southern Lipari [site number 14]. (c) Lithic-rich pumiceous deposits of the Falcone in

southern Lipari [site number 14]. (d) Monte Guardia pumiceous pyroclastic succession of pumice fall in NW Lipari [site number 13]; subdivided into the U1-U4 units; Monte Guardia is interbedded between two brown tuff deposits, just above the Lower Pollara tephra of Salina. (e) Vallone del Gabellotto pumice deposits in the area of Monte St. Angelo central Lipari [site number 12]. (f) Monte Pilato pumice and ash deposits from Monte St. Angelo, central Lipari [site number 11], they are divide into a lower Monte Pilato 1 (MP1) and Upper Monte Pilato 2 (MP2) layers. (g) Lami pumice deposits on Lipari (site number 10). (h) Quadrara deposits in southwest Vulcano [site number 9], typically characterised by a pumice layer vertically passing to a scoria blanket. (i) Palizzi B pumice deposits resting on the Palizzi A deposits inside the La Fossa caldera [site number 5]. (j) Varicoloured ash deposits of the Commenda on Vulcano [site number 3]. (k) Upper Pollara pumice deposits (corresponding to the ERU1 eruption unit) on Salina [site number 15]. (l) Upper Pollara pumice deposits (corresponding to the ERU 3 eruption unit NW Salina [site number 15]. (m) Lower Pollara scoria and pumice (Salina) on Lipari [site number 13] intercalated between different Brown Tuff deposits, underlying the Monte Guardia deposit. (n) Scoria and pumice of the Lower Pollara deposits near Valdichiesa, Salina [site number 16], outcropping above a Brown Tuff layer. (o) Upper Vancori pumice deposits in north-west Stromboli [site number 19]. (p) Secche di Lazzaro succession situated along the Semaforo Labronzo Track, northern Stromboli [site number 17], subdivided into five successive units.

Figure 3: Major element glass geochemical variations of the tephra units included in this study. (a) SiO_2 vs K_2O classification diagram and (b) TAS classification diagram. Error bars represented 2*standard deviations of replicated analyses of the StHs6/80-G secondary standard glass. In the legend the units are listed for each island according to their stratigraphic positions. Also shown are the compositions of distal tephra layers from the central Mediterranean marine (Paterne et al., 1988; Albert et al., 2012; Matthews et al., 2015; Insinga et al. 2014) and lacustrine (Narcisi, 2002) archives that are considered here for proximal-distal correlations to either Vulcano or Stromboli. Compositional fields are drawn

for the Intermediate Brown Tuffs (IBT [Gelso, Vulcano]), and the Upper Brown Tuffs [UBT, TGR Sup. Surge deposits, Vulcano] are based on selected glass data from Vulcano (Lucchi et al. 2008).

Figure 4: Average mantle normalised (Sun and McDonough, 1989) trace element profiles of Aeolian Island glasses. (a) rhyolitic glasses erupted on Lipari (Punta del Perciato, Falcone, Monte Guardia, Vallone del Gabellotto, Monte Pilato and Lami); Vulcano (Palizzi B, Upper Pietre Cotte) and Salina (Upper and Lower Pollara); (b) SHO and KS glasses erupted on Stromboli and Vulcano.

Figure 5: Major and trace element bi-plots of glasses for investigated tephra units erupted during approximately the last 21ka on Vulcano and Stromboli. Also shown are the compositions of distal tephra layers from the central Mediterranean marine (Paterne et al., 1988; Albert et al., 2012; Matthews et al., 2015; Insinga et al., 2014) and lacustrine (Narcisi, 2002) archives that are considered here for proximal-distal correlations. Error bars represented 2* standard deviations of replicated analyses of the StHs6/80-G secondary standard glass.

Figure 6: Major and trace element geochemical bi-plots of Lipari glasses during approximately the last 50 ka. A chemostratigraphic succession of Th content of the glasses is also shown (in brown are shown the intercalated layers of Brown Tuff). The subdivisions of individual tephra units conform to the descriptions provided in **Supplementary material 1**. Error bars represented 2* standard deviations of replicated analyses of the StHs6/80-G secondary standard glass. The Rocche Rosse lava flow composition is taken from Forni et al. (2013).

Figure 7: Major and trace element bi-plots of glasses of the investigated Salina tephra units. Subdivisions of the Upper Pollara succession into ERU1-5 eruption units are shown (conforming to Supplementary material 1), together with the samples of the Lower Pollara on Salina (Valdichiesa) and Lipari ("key-bed"). Also presented is the average composition of

the distal E-2 marine tephra from Paterne et al. (1988). Error bars represented 2* standard deviations of replicated analyses of the StHs6/80-G secondary standard glass.

Figure 8: Major element geochemical bi-plots of glasses for some of the investigated tephra units erupted during approximately the last 21 ka on Vulcano and Stromboli. The subdivision of individual tephra units conform to the descriptions provided in **Supplementary material 1**. Also presented are new glass data for distal tephra layers considered for proximal-distal correlations, along with the T-3 tephra from Lago Pergusa (Sicily; Narcisi, 2002). [a] Type-locality glass data for the Secche di Lazzaro (Stromboli) is included from Petrone et al. (2009) for comparisons with our data-sets derived at other localities on the island of Stromboli. Error bars represented 2* standard deviations of replicated analyses of the StHs6/80-G secondary standard glass.

Figure 9: Proximal-distal correlations for the Monte Guardia, Falcone and Punta del Perciato tephra units on Lipari. The subdivisions of individual tephra conform to the descriptions in **Supplementary material 1**. Also presented are distal tephra layers from the central Mediterranean considered as possible distal equivalents (see text for references). Error bars represented 2* standard deviations of replicated analyses of the StHs6/80-G secondary standard glass.

Figure 10: Proximal-distal tephra correlations for the Vallone del Gabellotto, Monte Pilato and Lami tephra deposits of Lipari. Subdivisions of individual tephra conform to descriptions in Supplementary material 1. Also presented are distal tephra layers from the central Mediterranean archives considered as possible distal equivalents, including two newly identified cryptotephra layers from the Ionian Sea core M25/4-12. The Rocche Rosse lava composition is taken from Forni et al. (2013).

Figure 11: Composite proximal-distal explosive event stratigraphy for the Aeolian Islands during approximately the last 50 ka. Arrows display age uncertainties. V=Vulcano; St=Stromboli; P=Panarea; L=Lipari; CM=Capo Milazzo, Sicily. Tie lines between the

proximal and distal setting are colour co-ordinated, red = Salina, blue = Lipari, green = Vulcano and black = Stromboli. The thick black lines are for distal tephra units of Campanian origin. For discussions see the text. Bold lettering denotes distal tephra correlations confirmed by new data in this study. The Ischia tephra is reported in Lucchi et al. (2013b) and is more recently correlated to the Monte Epomeo Green Tuff (Ischia) and the Y-7 marine tephra dated at c. 55 ka (Albert, 2012; Tomlinson et al. 2014; and references therein).

Table 1

Island	Eruptive Epochs (EE)	Eruptive history - summary of main volcanic-tectonic events/periods of quiescence/palaeoshore lines	Age (ka)	Compositions (Whole-rock classificaitons)
Vulcano (De Astis et al. 2013a, b; and references therein)	8	Effusive (Punta Nere, Palizzi) to Vulcanian (Pietre Cotte) to sub-Plinian (Palizzi) activity within the La Fossa caldera and construction of the La Fossa cone (last eruption 1888-1890); Strombolian (Vulcanello + Monte Saraceno). Dome activity (Monte Lentia)	8 ka - 1890 AD	SHO; Basaltic Trachy-andesite to rhyolite
		Collapse of La Fossa (between 13-8ka) + quiescence		
	7	Hydromagmatic activity in the La Fossa caldera + dome growth and coulee formation (Monte Lentia area; Casa Lentia)	20-13	SHO; Basaltic Trachy-andesite to rhyolite
		Partial caldera collapse of Piano caldera + quiescence		
	6	Dome growth and coulee formation (Monte Lentia area) + Strombolian activity along NW-SE eruptive fissures - scoria blankets (Spiaggia Lunga [24 ka] and Quadrara [21 ka]	28-21	SHO; Basalt to Rhyolite
		Caldera collapse of La Fossa + Quiescence	42-24	
	5	Piano Caldera infilling, hydromagmatic activity and some strombolian activity		SHO; Basalts
	4	Post collapse volcanic activity concentrated on caldera ring faults, fissure activity (hydromagmatic)		HKCA to SHO; Basalts
		Caldera collapse of La Fossa (c. 80 ka) + period of quiescence	80	
		Volcanic activity shifts North-westward		
	3	Post collapse volcanic activity concentrated on caldera ring faults, effusive		SHO; Basalt
		Primordial Vulcano Collapse (c. 100 ka) produced Piano caldera	ca.100	
	1-2	Primordial Vulcano stratocone construction, effusive to Strombolian activity	127-101	HKCA and SHO; Basltic Andesite and Trachy-andesites

Lipari (Forni et al., 2013; Lucchi et al., 2013b; and references therein)	9	NE shift of eruptive vents. Strombolian to sub-Plinian (Vallone del Gabellotto, Monte Pilato and Lami), effusive activity (Rocche Rosse; last activity on Lipari 1220 AD). Deposits interlayered within External Brown Tuff deposits thought to originate from with La Fossa caldera (Vulcano) External Brown Tuff deposits	8.7-1220 AD	HKCA, rhyolite
	8	Sub-Plinian (Monte Guardia), and dome type effusive activity (NNW-SSE aligned) in SW Lipari, separated by periods of sub-aerial erosion External Brown Tuff deposits	27 - > 8.7	HKCA, Dacite and Rhyolite
	7	Shift of eruptive vents to SW Lipari. Strombolian to sub-Plinian pyroclastic (Punta del Perciato and Falcone) interlayered between external Brown Tuff deposits. Also Dome type effusive activity and fissure activity (NNW-SSE aligned) External Brown Tuff deposits + Grey Porri Tuffs (Salina 67-70). MIS 5a marine erosion (palaeoshoreline terrace) and quiescence	56-40	HKCA, Dacite and Rhyolite
	6	M.S. Angelo and M. Chirca, effusive to vulcanian activity MIS 5c marine erosion (palaeoshoreline terrace)	92-81	HKCA - Andesite
	4-5	M. S. Angelo stratovolcano construction, hydromagmatic-effusive activity MIS 5e marine erosion (palaeoshoreline terrace)	119-105	CA to HKCA, Basalt to Dacite
	1-3	Hydromagmatic to strombolian - effusive activity - western Lipari along NNW-SSE to N-S tectonic trends Construction of the M. Chirca stratocone (EE3).	267-150	CA to HKCA
Salina (Lucchi et al., 2013a; and references therein)	6	Pollara crater (NW Salina), lava flow, followed by two highly explosive Vulcanian (Upper Pollara) to sub-Plinian (Lower Pollara) eruptions	30-15.6	CA to HKCA; Basalt to Rhyolite
	5	Monte dei Porri stratovolcano development, (western Salina), includes the Grey Porri Tuffs, strombolian to sub-Plinian (67-70ka) (West Salina) MIS 5e, MIS 5c MIS 5a marine erosion terraces (Last-interglacial)	ca. 70 - 56	CA; Basalt to Andesite
	3-4	Monte Rivi cone construction, and the Fossa delle Felci Stratovolcano, strombolian and effusive activity (Eastern Salina) MIS 7 marine erosion (palaeoshoreline terrace)	ca. 160-121	CA to HKCA; Basalt to Dacite
	1-2	Pizzo Capo volcano construction from fissure-type activity (Eastern Salina)	244-226	CA; Basalt
Stromboli (Francalanci	6	Recent Stromboli, present-day explosive activity developed since the 8th Century	2.4-present	SHO and HKCA; Basalt

et al., 2013; Rosi et al., 2013; references therein)	5	Neostromboli activities, effusive sheet lava flows, exposed along the shoulders of the Sciarra del Fuoco morphostructural scar, hydromagmatic explossive eruptions assosiated with major sector collapse of the Sciarra del Fuoco (Secche di Lazzaro pryroclastics) Vancori collapse	12-4	KS; Basaltic Trachy-andesite
	4	Vancori (Lower, Middle and Upper) stratocone construction, effusive and explosive (Upper Vancori) filling the caldera depression	<25-13	SHO; Basalt to Trachyte
		Prolonged quiescence - caldera development	41-34 to ca. 26	
	3	Palaeostromboli II stratocone construction; effusive and strombolian activity	41-34	HKCA to SHO
	2	Palaeostromboli II stratocone construction; effusive and strombolian activity	67-54	CA
	1	Palaeostromboli I stratocone construction; effusive and explosive deposits (Petrazza eruption; strombolian to sub-Pinian [77-75ka])	< 100 (85-75)	HKCA; Basalts to andesite

Table 2

Sample location(s)	Deposit characteristics and Activity	Sampled	mingled	Vent location	Dispersal		Glass Data Source	Age	UTM	
					Axis	Intra-Island/Capo Milazzo			X	Y
1	pdc and pumice lapilli fall; Vulcanian[1, 2, 3]	pumice	x	La Fossa	E [1]		This study	1731-1739 AD [1,2,3]	496258.43	4250813.10
2	scoria/pumice lapilli fall; Vulcanian/Strombolian (coeval activity with the second eruption of the Forgia eccentric vent)[1]	pumice/ scoria		La Fossa	N [1]		This study	1727 AD [1]	496714.28	4250398.44
2	scoria/pumice lapilli fall; Vulcanian/Strombolian[1]	scoria			NE [1]		This study	1626 AD [1]		
3	Stratified ash layers; either associated with; ash fallout and syn- /post-eruptive lahars [1, 4, 5] or turbulent and diluted pdc's; Vulcanian [6, 7]	ash		La Fossa	Radial [7]		This study	AD 918–1302 [8] (Breccia di Commenda lithics directly below Comm	496900.51	4249861.39

								enda Ash)	
4	Inversely graded, clast supported, pumice lapilli fall; Vulcanian/sub-Plinian[1, 5, 6, 7, 9]	pumice		La Fossa	S [1,5]		This study	Between	496900.51	496900.51
5	Inversely graded, clast supported, pumice lapilli fall; sub-Plinian[1, 5, 6, 7, 9]	pumice		La Fossa	W (Lentia) [1,5]		This study	2.1±0.3 and 1.5 ± 0.2 ka [7, 9, 10, 11]	496551.11	4249986.66
6	Densely laminated ash beds; either interpreted as representing ash fallout associated with long lasting phreatomagmatic mafic ash eruptions (+ laharic components) [1, 5] or dilute pdc deposits; Vulcanian[6, 7]	ash		La Fossa	Mainly SE [1,5]		Albert et al.(2012); This study	2100± 300 yrs BP [12]	496603.51	4250042.78
7	Massive ash (PDC), containing thin scoria beds (fall)[2, 6, 12]	scoria		Within Caldera La Fossa	S	Lipari [14]	Albert et al.(2012)	8,305-8,720 cal yr BP (7680± 100 ^{14}C yrs)[6]	498068.72	4248981.82
8	Clast supported pumice bombs† (fall)[15]	pumice		Lentia			This study	13 ± 1 Ka [16]	495152.94	4251241.45
9	Inversely graded, clast supported pumice lapilli (fall) passing upwards into a welded scoriaeous blanket †; sub-Plinian [15]	pumice and scoria	x	SW Vulcano	S[17]	Capo Milazzo[17]	This study	21 ± 3.4 Ka [18]	498672.81	4247022.02
10	Alternating clast supported obsidian-rich pumice lapilli (fall) and poorly sorted and ash-supported with lenses of pumice lapilli (PDC)[19]; Vulcanian; *possibly coeval with the	pumice and ash		Monte Pilato/Rocche Rosse	?	Vulcano (Vulcanello), Panarea,	This study	0.70 ± 0.17 ka[22]	-	-

	Roche Rosse Lava flow[20]					Stromboli [13, 14, 21]				
11	Ash beds and clast supported pumice lapilli (fall) [23]; divided into two temporally disinct eruptive units MP1 and MP2[13]; sub-Plinian	pumice		Monte Pilato	S [7]		Albert et al.(2012); This study	776 AD or 1,076-1,266 cal yrs BP (^{14}C 1241±31 yrs BP)[23]	494617.02	4260022.53
12	Plane parallel to cross-bedded pumice lapilli deposits (PDCs) with minor clast supported fall deposits †; sub-Plinian[24, 25]	pumice		Vallone Gabellotto	NE, E, S [21, 26]	Vulcano, Panarea[21]	This study	8,430-8,730 cal yrs BP (^{14}C7770±70 yrs BP)[26]	494419.59	4260043.72
13	Clast supported pumice lapilli fall and alternating ash and lapilli (rounded) tuff beds (PDCs)†; sub-Plinian[24, 28]	pumice	x	Monte Guardia	N, S & E	Vulcano[14, 21], Panarea[21,29]	This study	24,650 - 27,100 cal yrs BP [17, 27,30, 20, 31, This Study]	493190.00	4259983.00
14	Pumiceous lapilli tuffs (PDCs); sub-Plinian? [25, 32]	pumice	x	Southern Domes			This study	40-43 ka[20]	494267.87	4257017.33
14	Clast supported pumice lapilli fall, with interbedded ash/lapilli layers (PDCs); sub-Plinian? [25, 32]	pumice		Southern Domes			This study	< 55 ka[20]	494267.87	4257017.33

No.	Description	Composition		Location	Dir.	Source	Reference	Age		
15	Poorly sorted, pumice lapilli deposits (PDCs); Vulcanian [32, 33]	pumice	x	Pollara Crater			This study	15,000 - 16,090 cal yrs BP (^{14}C 12970 ±180 yrs BP)[34]	484130.43	4270016.82
13[KB], 16	Well sorted, clast supported scoria passing to well sorted pumice (fall)†; sub-Plinian [33,34,35]	scoria and pumice	x	Pollara Crater	SE [34, 36]	Lipari [13, 14, 21, 31]	Albert et al.(2012); This study	26,410 - 27,630 cal yrs BP [17, 27, 30, 20, 31, 33, This Study]	[KB]493190.00 [16]4851122.00	4259983.00 42678 34.00
17 (N)	Bedded ash and sorted scoria lapilli (fall). Accretionary lapilli observed. Capped by poorly sorted laharic deposit containing pumice lapilli†; phreatomagmatic/sub-Plinian [36, 37]	scoria and pumice		Stromboli Summit			Albert et al.(2012); This study	5-7 ka [38]/ 7 ka [37]	518687.63	4294937.43
18 [NE)	Laminated ash beds (fall). Poorly sorted ash and lapilli beds (PDCs). The sequence is capped by laharic deposits†; phreatomagmatic[37, 39]	pumice		Stromboli Summit; plus local vent?			Albert et al.(2012); This study		520260.65	4294887.82
19	Clast supported pumice beds, with intervening ash unit (fall)†; Vulcanian/sub-Plinian[38]	pumice		Vancori, Summit	NE		This study	13 ka [37]	520636.6	4294712.5

Table 3

Source	Vulcano Island									
Tephra	Upper Pietre Cotte		Lower Pietre Cotte		Comenda Ash	Palizzi D	Palizzi B		Palizzi A	
Locality	1		2		3	4	5		6	
Clast I.D.	S90cb.7.4	AT1.w3.2	LPC1.2.2	LPC1.10.2	CA5.21	S33-15.g2	VULC46.1.2	VULC46.7.3	S77-b.1.1	S77-e.4.1
Material (wt.%)	pumice	pumice	scoria	scoria	ash	pumice	pumice	pumice	scoria	scoria
SiO_2	59.78	73.19	57.62	59.10	60.98	60.41	71.55	72.67	56.05	57.81
TiO_2	0.58	0.19	0.70	0.55	0.49	0.53	0.17	0.20	0.64	0.61
Al_2O_3	17.68	13.23	16.95	17.82	17.39	18.39	14.12	13.27	18.43	17.30
FeOt	5.76	2.42	6.16	5.84	5.26	4.37	2.54	2.36	6.66	6.57
MnO	0.03	0.08	0.19	0.10	0.12	0.11	0.09	0.06	0.14	0.12
MgO	1.22	0.20	2.61	1.40	1.22	0.97	0.18	0.16	2.02	1.77
CaO	2.91	0.80	5.47	3.47	2.90	2.52	0.81	0.87	4.59	3.86
Na_2O	4.82	3.82	4.24	4.67	4.56	4.82	3.45	3.46	4.52	4.79
K_2O	7.21	6.07	6.06	7.06	7.07	7.89	7.09	6.95	6.94	7.17
Total	97.79	95.81	98.90	98.93	98.05	99.11	96.11	95.58	97.55	96.02

Source	Vulcano Island							Lipari Island	
Tephra	Upper Tufi di Grotte dei Rossi (scoria)		Casa Lentia		Quadrara				Lami	
Locality	7		8		9				10	
Clast I.D.	5A	12B	9B	1A	U1-9B	U2-19D	U3-1A	U4-18D	09-5/U4	005-6/U9
Material	scoria	scoria	pumice	pumice	pumice	pumice	scoria	scoria	pumice	pumice

(wt.%)										
SiO$_2$	54.37	57.44	68.68	70.49	63.63	63.45	60.23	58.12	74.62	75.10
TiO$_2$	0.70	0.61	0.37	0.30	0.36	0.43	0.56	0.71	0.09	0.09
Al$_2$O$_3$	16.33	17.23	15.19	14.88	18.02	17.23	18.23	18.33	13.27	13.16
FeOt	8.80	7.08	3.32	2.73	3.67	4.01	5.29	6.54	1.55	1.53
MnO	0.10	0.09	0.14	0.12	0.10	0.19	0.12	0.13	0.00	0.06
MgO	3.98	2.31	0.48	0.47	0.88	0.97	1.71	2.28	0.08	0.02
CaO	7.72	4.98	1.42	1.21	2.98	2.75	4.40	5.39	0.71	0.69
Na$_2$O	3.63	4.33	3.99	3.73	4.59	4.72	4.45	3.59	4.41	4.25
K$_2$O	4.37	5.91	6.41	6.06	5.77	6.25	5.01	4.91	5.28	5.11
Total	98.37	98.79	97.94	98.62	98.11	95.25	96.25	97.49	96.35	97.53

Source	**Lipari Island**									
Tephra	Monte Pilato 2 (upper)		Mont Pilato 1 (lower)		Vallone del Gabellotto			Monte Guardia		
Locality	11		11		12			13		
Clast I.D.	7B	15C	4A	10B	U2-8B	U5-10B	U8-10B	U1a-14C	U1a-17D	U1d-5A
Material	pumice	pumice	pumice	pumice	pumice	pumice	pumice	pumice	pumice	pumice
(wt.%)										
SiO$_2$	75.55	75.37	76.07	75.99	75.38	75.38	75.10	76.41	72.51	76.58
TiO$_2$	0.08	0.08	0.05	0.07	0.07	0.01	0.09	0.03	0.18	0.04
Al$_2$O$_3$	12.71	13.16	12.63	12.66	13.28	13.33	13.20	12.46	15.03	12.73
FeOt	1.56	1.52	1.37	1.42	1.65	1.54	1.61	1.43	1.83	1.26
MnO	0.11	0.13	0.06	0.00	0.18	0.03	0.08	0.06	0.00	0.14
MgO	0.00	0.04	0.02	0.03	0.03	0.02	0.03	0.02	0.10	0.00
CaO	0.71	0.77	0.76	0.63	0.72	0.76	0.77	0.60	0.99	0.65
Na$_2$O	4.01	3.71	3.95	4.18	3.67	3.77	3.94	3.54	3.41	3.67
K$_2$O	5.28	5.23	5.09	5.01	5.01	5.15	5.18	5.45	5.95	4.93

Total	98.62	98.94	96.32	97.30	98.01	97.64	97.83	96.49	94.98	96.82

Source	**Lipari Island**							**Salina Island**		
Tephra	Monte Guardia			Falcone		Punta del Perciato		Upper Pollara		
Locality		13			14		14		15	
Clast I.D.	U1d-9B	U3e-9B	U4-15C	7B	15C	3A	14C	ERU1-4A	ERU1-14C	ERU2-8B
Material (wt.%)	pumice	pumice	pumice	pumice	pumice	pumice	pumice	pumice	pumice	pumice
SiO_2	74.54	75.92	76.12	73.90	76.28	76.35	76.47	71.72	74.42	74.54
TiO_2	0.11	0.10	0.04	0.19	0.06	0.07	0.04	0.32	0.27	0.25
Al_2O_3	13.54	12.76	12.79	14.41	12.44	12.55	12.36	15.07	14.01	13.70
FeOt	1.83	1.43	1.27	1.68	1.50	1.29	1.16	2.22	1.56	1.66
MnO	0.07	0.04	0.04	0.03	0.05	0.03	0.14	0.10	0.09	0.04
MgO	0.10	0.01	0.01	0.07	0.01	0.00	0.01	0.48	0.30	0.37
CaO	0.75	0.70	0.67	0.88	0.72	0.70	0.69	2.77	1.93	1.93
Na_2O	2.89	3.81	3.97	3.06	3.33	3.25	3.37	3.71	3.52	3.70
K_2O	6.15	5.24	5.10	5.79	5.60	5.75	5.77	3.60	3.89	3.81
Total	94.65	96.27	95.71	94.93	95.34	96.22	95.64	97.91	96.35	95.67

Source	**Salina Island**									
Tephra	Upper Pollara					Lower Pollara				
Locality			15				13			16
Clast I.D.	ERU3-13C	ERU4-15C	ERU4-7C	ERU5-3A	ERU5-8B	KB'-4A	KB-6B	KB-9B	LP_U3_14C	LP_U3_11C
Material (wt.%)	pumice	pumice	pumice	pumice	pumice	pumice	pumice	pumice	pumice	pumice
SiO_2	75.56	72.95	75.76	72.05	75.09	68.21	70.13	74.14	69.16	72.18

TiO_2	0.16	0.31	0.18	0.27	0.24	0.38	0.33	0.24	0.43	0.30
Al_2O_3	14.30	14.47	13.64	15.41	13.87	15.94	15.25	14.26	15.34	14.79
FeOt	1.08	2.11	1.03	1.97	1.04	3.60	3.24	1.85	3.33	2.53
MnO	0.06	0.04	0.08	0.00	0.19	0.07	0.02	0.05	0.07	0.04
MgO	0.21	0.35	0.19	0.39	0.26	1.02	0.83	0.38	0.91	0.54
CaO	1.28	2.01	1.33	2.74	1.44	4.09	3.30	1.92	3.72	2.41
Na_2O	3.19	3.84	3.83	3.79	3.92	3.84	3.82	3.82	4.10	3.87
K_2O	4.16	3.91	3.96	3.37	3.96	2.85	3.08	3.33	2.93	3.34
Total	95.36	95.79	94.66	95.70	94.51	96.34	98.61	95.16	96.98	95.80

Source	Salina Island	Stromboli Island								
Tephra	LP	Secche di Lazzaro					Upper Vancori			
Locality	16	17		18			19			
Clast I.D.	U3_7B	U2-11C	U5-1A	U3-5 A	U4-6B	U4-18D	U1-1A	U1-8B	U3-12C	U3-15C
Material (wt.%)	pumice	scoria	pumice	pumice	pumice	pumice	pumice	pumice	pumice	pumice
SiO_2	74.89	57.86	59.27	59.36	60.10	59.82	65.21	64.74	63.64	64.00
TiO_2	0.24	1.10	0.93	0.97	1.03	0.89	0.79	0.75	0.75	0.82
Al_2O_3	14.04	18.01	17.88	17.66	17.08	17.46	16.32	16.43	16.57	16.50
FeOt	1.47	6.48	5.58	5.77	5.46	5.45	4.39	4.28	4.55	4.46
MnO	0.09	0.15	0.17	0.18	0.20	0.12	0.13	0.17	0.20	0.17
MgO	0.31	1.96	1.60	1.62	1.65	1.67	0.84	0.93	1.20	1.13
CaO	1.65	4.65	3.85	4.17	3.84	4.02	2.34	2.61	2.86	3.05
Na_2O	4.05	3.30	3.87	3.72	3.72	3.81	4.40	4.64	4.75	4.35
K_2O	3.26	6.49	6.85	6.54	6.92	6.77	5.59	5.46	5.48	5.50
Total	96.03	98.45	98.50	98.14	97.98	98.53	99.37	99.10	99.31	97.53

Table 4

Vulcano Island

Source Tephra	Upper Pietre Cotte		Lower Pietre Cotte		Commenda Ash	Palizzi D		Palizzi B		Palizzi A		Upper Tufi di Grotte dei Rossi (scoria)		Casa Lentia	Quadrara			
Locality	1		2		3	4		5		6		7		8	9			
Sample	S90ca.4	AT1.w2	LPC1.7	LPC1.5	CA5.12	110.15	110.9	46.1	46.14	S77e.2	S77b.10	3A	12C	7B	U1-9B	U2-17D	U3-5A	U4-13C
Material	pumice	pumice	scoria	scoria	ash	pumice	pumice	pumice	pumice	scoria	scoria	scoria	scoria	pumice	pumice	pumice	scoria	scoria
TAS	Tra	Rhy	Tra	Tra	Tra	Pho-Tra	Pho-Tra	Rhy	Rhy	TP-Pho	TP-Pho	Bas-TraA	TraA	Tra-Rhy	Tra	Tra	TraA	TraA
V	102	23	33	33	85	46	50	3	5	153	132	256	202	51	72	50	145	144
Rb	280	414	431	424	256	253	254	319	332	222	230	147	201	323	181	201	154	161
Sr	712	87	953	836	774	628	718	35	44	827	934	1189	972	183	806	900	1182	1220
Y	23.4	39.7	25.4	28.6	22.9	17.7	18.6	36.0	36.7	20.5	20.6	19.2	20.7	31.1	28.1	27.4	24.6	23.2
Zr	256	297	306	337	274	193	209	173	201	190	199	121	162	206	213	213	155	162
Nb	32.8	45.8	49.0	53.3	32.3	28.6	30.4	35.6	38.0	26.8	28.1	16.5	21.9	36.5	24.1	24.4	18.3	18.0
Ba	1151	111	1748	1534	1030	1281	1435	53	81	1153	1283	803	925	410	947	1064	1074	1079
La	77.8	96.4	111.1	126.0	78.3	55.4	60.3	67.3	78.8	68.2	72.2	46.2	60.1	60.9	60.1	63.3	52.3	51.5
Ce	139.3	179.2	204.4	226.2	140.6	97.3	107.7	124.8	144.6	125.1	131.0	88.3	107.2	118.2	119.5	113.9	100.7	101.0
Pr	13.7	17.4	19.7	22.6	13.5	9.5	10.7	12.4	14.4	12.9	12.9	9.7	11.1	12.1	13.	12.0	10.4	11.0

Nd	48.2	62.2	69.4	77.6	47.3	33.3	36.4	42.1	47.4	47.8	46.2	35.9	42.0	43.6	45.0	45.1	44.1	44.2
Sm	8.1	9.8	12.0	13.6	7.5	6.5	6.5	7.1	8.7	7.8	8.1	6.7	7.7	7.8	8.9	8.5	8.2	7.9
Eu	1.5	0.5	2.2	2.5	1.3	1.2	1.5	0.2	0.3	1.6	1.4	1.5	1.5	0.7	1.5	1.8	1.9	1.7
Gd	5.7	7.3	9.7	10.5	5.4	5.3	5.0	6.3	6.8	6.7	6.1	5.6	5.4	5.5	6.0	6.7	6.7	6.3
Dy	4.1	6.2	5.9	6.5	4.2	3.3	3.3	6.1	6.5	3.9	4.3	3.9	4.6	5.5	4.9	4.9	4.8	5.0
Er	2.1	4.0	3.3	3.5	2.3	1.7	1.9	3.8	4.0	2.0	2.3	1.9	2.1	3.2	2.6	2.7	2.5	2.5
Yb	2.7	4.3	3.9	4.3	2.6	2.3	2.1	4.2	4.4	2.2	2.3	2.0	2.5	3.6	2.6	2.6	2.6	2.5
Lu	0.4	0.7	0.7	0.7	0.4	0.4	0.4	0.6	0.6	0.4	0.4	0.3	0.3	0.5	0.4	0.4	0.4	0.3
Ta	1.9	2.5	3.0	2.9	1.9	1.6	1.6	2.5	2.6	1.5	1.6	0.9	1.2	2.5	1.4	1.2	1.0	0.9
Th	39.5	60.5	60.7	63.1	41.1	28.8	32.5	52.5	58.0	31.8	32.7	18.3	26.7	47.9	24.1	23.9	18.0	18.6
U	12.0	19.8	18.6	19.8	12.5	9.4	9.7	16.3	17.5	9.3	10.4	5.9	8.1	14.6	8.3	6.8	5.6	5.5

Source							**Lipari Island**											
Tephra	Lami	M. Pilato 2	M. Pilato 1	Vallone del Gabellotto			Monte Guardia								Falcone		Punta del Perciato	
Locality	10	11	11	12			13								14		14	
Sample	U10-006-6	10 B	10B	U2-12C	U5-12C	U8-11C	U1a-6B	U1a-3A	U1d-3A	U1d-12C	U3e-9B	U3e-15C	U4-12C	U4-13C	3A	15C	2A	8B
Material	pumice	pumice	pumice	pumice	pumice	pumice	pumice	pumice	pumice	pumice	pumice	pumice	pumice	pumice	pumice	pumice	pumice	pumice
TAS	Rhy	Rhy	Rhy	Rhy	Rhy	Rhy	Rhy	Rhy	Rhy	Rhy	Rhy	Rhy	Rhy	Rhy	Rhy	Rhy	Rhy	Rhy
V	<LOD	<LOD	<LOD	<LOD	<LOD	<LOD	<LOD	<LOD	<LOD	<LOD	<LOD	<LOD	<LOD	<LOD	<LOD	<LOD	<LOD	<LOD
Rb	312	331	326	314	311	322	314	297	308	301	299	292	297	303	315	327	310	319

Sr	16.6	16.9	16.0	15.2	15.9	16.8	7.9	7.8	7.9	9.5	8.9	8.5	7.7	8.0	9.1	9.5	8.3	8.8
Y	38.1	42.6	38.0	39.8	40.4	40.8	33.9	37.3	40.1	35.5	35.0	38.8	37.7	38.9	37.6	39.9	38.0	39.3
Zr	183	182	164	172	172	171	115	124	136	125	115	122	124	127	127	118	118	121
Nb	40.3	38.9	35.4	37.0	36.7	36.7	32.1	33.3	35.2	32.8	32.2	33.4	34.6	33.9	34.4	34.1	34.2	34.4
Ba	19.2	16.3	14.5	15.1	16.2	15.4	5.4	3.9	4.1	4.1	7.9	4.0	4.1	4.2	4.1	3.7	3.3	3.6
La	62.8	57.7	53.1	53.8	54.6	55.5	32.7	34.0	36.9	32.9	31.1	35.8	35.5	36.0	37.5	33.2	35.3	34.9
Ce	128.6	116.0	107.6	107.4	110.7	110.6	70.3	75.2	80.5	71.0	69.7	78.0	74.7	76.4	80.2	75.1	74.1	76.3
Pr	<LOD	11.8	10.9	11.2	11.7	11.9	7.8	8.3	9.1	8.1	8.1	8.6	8.3	8.5	8.9	8.1	8.4	8.2
Nd	42.8	43.2	38.9	38.8	39.8	40.0	31.8	31.5	34.1	30.5	29.8	33.8	31.4	32.0	35.8	32.6	33.1	33.5
Sm	<LOD	9.2	8.7	8.5	8.3	9.2	6.7	7.6	8.3	6.2	7.2	7.1	7.3	7.5	8.4	7.6	7.9	8.4
Eu	<LOD	0.2	0.1	0.2	0.3	0.3	0.2	0.1	<LOD	<LOD	0.6	0.3	<LOD	0.1	0.3	0.2	0.2	0.3
Gd	<LOD	7.0	6.5	6.5	7.0	6.7	5.3	6.0	6.4	6.1	5.7	6.1	6.6	6.0	5.5	6.5	6.6	6.5
Dy	<LOD	7.4	6.6	6.9	6.8	6.8	5.7	6.5	6.7	5.9	6.2	6.6	6.8	6.6	6.7	6.6	6.2	6.6
Er	4.4	4.5	4.1	4.2	4.3	4.4	3.6	3.9	4.4	3.7	3.8	3.9	3.8	4.1	4.0	4.3	3.9	4.0
Yb	<LOD	5.1	4.5	4.7	4.9	4.9	4.0	4.5	5.1	4.1	3.7	4.5	4.3	4.5	4.3	4.6	4.5	4.7
Lu	n.d	0.7	0.7	0.7	0.7	0.7	0.6	0.7	0.7	0.6	0.6	0.7	0.7	0.6	0.7	0.7	0.6	0.6
Ta	2.8	2.7	2.3	2.4	2.5	2.6	2.1	2.3	2.5	2.4	2.0	2.2	2.2	2.3	2.4	2.1	2.4	2.3
Th	53.1	53.6	47.9	51.1	49.9	51.8	35.0	38.9	42.6	37.7	36.2	40.0	39.0	41.5	39.7	37.7	39.2	39.9
U	16.7	16.6	14.9	15.3	15.8	16.0	11.8	12.8	13.5	12.6	12.3	12.4	12.8	13.0	12.8	12.3	13.2	13.5
Source	Salina Island						Stromboli Island											
Tephra	Upper Pollara			Lower Pollara			Secche di Lazzaro										Upper Vancori	

Locality	15				13			16		17				18		19		
Sample	ERU1-6B	ERU2-6B	ERU3-20D	ERU4-9B	LP13-20-2A	LP13-20-6B	LPUpper-14C	U3-2A	U3-8B	U2-1A	U2-10B	U5-6B	U5-7B	U3-5A	U4-5A	U1-1A	U1-6B	U3-7B
Material	pumice	pumice	pumice	pumice	pumice	pumice	pumice	pumice	pumice	Scoria	Scoria	pumice	pumice	pumice	pumice			
TAS	Rhy	Rhy	Rhy	Rhy	Rhy	Rhy	Rhy	Rhy	Rhy	*TraA*	*TraA*	Tra	Tra	Tra	Tra	Tra	Tra	Tra
V	<LOD	<LOD	<LOD	<LOD	<LOD	<LOD	<LOD	<LOD	<LOD	164	173	135	123	142	141	21	22	48
Rb	93	130	130	129	103	92	103	96	95	286	275	287	249	274	288	180	187	196
Sr	544	298	302	288	308	415	308	289	307	540	586	488	516	481	463	349	232	357
Y	14.9	13.7	16.2	14.9	11.2	12.3	12.0	11.0	10.4	24.0	28.6	29.3	24.6	27.5	24.2	29.1	28.7	31.4
Zr	110	113	136	127	138	115	143	128	140	255	289	307	261	289	339	297	296	322
Nb	13.4	15.3	17.9	17.1	13.3	11.0	13.7	13.0	13.8	37.2	40.2	43.1	36.0	41.2	47.4	37.4	36.3	38.3
Ba	1160	1268	1396	1352	978	895	980	949	979	2077	2161	2251	2165	2194	2012	1446	1248	1535
La	38.6	41.3	44.8	43.5	32.1	29.0	31.9	31.4	33.1	62.4	66.3	69.1	58.8	64.6	49.7	58.8	57.8	65.4
Ce	66.9	67.8	75.8	73.7	56.1	54.1	54.4	49.7	53.7	123.8	129.8	136.5	115.5	128.0	96.2	111.7	111.0	126.2
Pr	6.3	5.9	6.5	6.4	5.3	5.7	5.2	4.8	4.8	13.3	13.8	14.3	11.9	13.9	10.7	11.3	11.4	13.1
Nd	21.5	18.8	23.7	20.9	16.2	17.0	17.0	16.1	15.2	49.2	53.9	56.1	45.4	50.9	40.1	42.0	40.9	48.0
Sm	<LOD	3.6	4.2	3.7	3.0	4.4	2.8	<LOD	<LOD	9.5	9.7	10.8	8.3	8.9	7.4	7.4	7.6	9.1
Eu	1.0	0.7	0.9	0.7	0.7	0.8	0.7	<LOD	0.9	2.0	2.2	1.9	1.8	2.0	2.0	1.8	1.4	1.7
Gd	<LOD	<LOD	2.5	2.7	2.2	2.8	1.9	<LOD	<LOD	6.5	7.3	6.3	6.9	6.7	5.5	6.4	5.4	7.0

Dy	2.5	2.1	2.4	1.9	1.9	2.3	1.9	<LOD	2.1	5.0	5.5	5.5	4.7	5.1	4.8	4.9	4.9	5.6
Er	1.7	1.4	1.5	1.5	1.3	1.4	1.3	<LOD	<LOD	2.6	2.8	3.1	2.5	2.8	2.4	2.9	2.9	3.7
Yb	1.9	2.0	2.2	2.1	1.8	1.6	1.8	<LOD	<LOD	2.2	2.6	3.0	2.7	2.7	2.4	3.2	3.1	4.0
Lu	<LOD	<LOD	0.3	0.3	0.3	0.3	0.3	<LOD	<LOD	0.3	0.4	0.4	0.4	0.4	0.4	0.5	0.5	0.6
Ta	0.9	0.9	0.9	0.8	0.7	0.6	0.8	0.9	0.8	1.9	2.1	2.2	1.8	2.3	2.5	1.9	1.9	2.1
Th	13.0	15.7	19.6	18.3	12.1	10.8	13.3	10.6	12.1	29.3	32.5	35.0	28.8	32.5	32.1	31.1	29.9	32.1
U	4.5	4.9	5.5	5.7	4.2	3.6	4.0	3.3	3.9	10.0	9.8	10.9	9.1	10.5	10.5	8.6	8.6	8.9

Table 5

Island	Vulcano										
Eruption	U. Pietre Cotte		L. Pietre Cotte	Commenda Ash	Palizzi D	Palizzi B	Palizzi A	Upper Tufi di Grotte dei Rossi (scoria)	Casa Lentia	Quadrara	
Sample Loc.	1	1	2	3	4	5	6	7	8	9	
Sampled	pumice	pumice	pumice/scoria	ash	pumice	pumice	ash	scoria	Pumice	scoria	pumice
TAS	Trachyte*	Rhyolite†	Trachyte*	Trachyte*	Trachyte*	Rhyolite†	Trachyte*	B. Tra-And*	Tra-Rhyolite†	Tra-Andesite†	Trachyte†
Nb/Zr	0.13 ± 0.01	0.15 ± 0.02	0.16 ± 0.01	0.12 ± 0.01	0.15 ± 0.02	0.20 ± 0.03	0.14 ± 0.01	0.13 ± 0.01	0.18 ± 0.01	0.11 ± 0.01	0.11 ± 0.01
Nb/Th	0.85 ± 0.05	0.79 ± 0.09	0.83 ± 0.07	0.81 ± 0.05	0.97 ± 0.16	0.68 ± 0.13	0.87 ± 0.04	0.88 ± 0.05	0.75 ± 0.03	0.98 ± 0.07	1.02 ± 0.12
Ta/Th	0.05 ± 0.01	0.04 ± 0.01	0.05 ± 0.01	0.05 ± 0.003	0.06 ± 0.01	0.05 ± 0.01	0.05 ± 0.003	0.05 ± 0.01	0.05 ± 0.005	0.06 ± 0.01	0.06 ± 0.01
Zr/Th	6.6 ± 0.3	5.4 ± 1.3	5.2 ± 0.4	6.7 ± 0.19	6.6 ± 0.6	3.3 ± 0.4	6.1 ± 0.3	6.6 ± 0.6	4.3 ± 0.2	8.7 ± 0.3	9.1 ± 1.0
La/Yb	29.8 ± 4.2	29.5 ± 20.0	30.4 ± 7.5	30.9 ± 1.6	25.2 ± 8.8	19.4 ± 6.4	30.1 ± 4.6	24.6 ± 3.6	16.3 ± 3.2	20.7 ± 3.0	22.1 ± 2.4

Island	Lipari							Salina		
Eruption	Lami	Monte Pilato 2 (Upper)	Monte Pilato 1 (Lower)	Vallone del Gabellotto	Monte Guardia	Falcone	Punta del Perciato	Upper Pollara	Lower Pollara	
Sample Loc.	10	11	11	12	13	14	14	15	13 (KB)	16
Sampled	pumice	pumice	pumice	pumice	pumice pumice	pumice	pumice	pumice	pumice	pumice
TAS	Rhyolite	Rhyolite	Rhyolite	Rhyolite	Rhyolite	Rhyolite	Rhyolite	Rhyolite	Dacite-Rhyolite	
Nb/Zr	0.22 ±	0.22 ± 0.01	0.22 ± 0.01	0.22 ± 0.01	0.27 ± 0.01	0.28 ±	0.28 ± 0.02	0.13 ±	0.09 ± 0.1	0.10 ±

	0.02					0.03		0.01		0.01
Nb/Th	0.74 ± 0.07	0.73 ± 0.03	0.74 ± 0.05	0.74 ± 0.04	0.86 ± 0.07	0.88 ± 0.05	0.88 ± 0.04	0.93 ± 0.06	1.05 ± 0.11	1.16 ± 0.13
Ta/Th	0.05 ± 0.01	0.05 ± 0.004	0.05 ± 0.003	0.05 ± 0.004	0.06 ± 0.005	0.06 ± 0.006	0.06 ± 0.005	0.05 ± 0.01	0.06 ± 0.01	0.07 ± 0.1
Zr/Th	3.4 ± 0.2	3.4 ± 0.1	3.4 ± 0.1	3.4 ± 0.1	3.2 ± 0.2	3.2 ± 0.4	3.1 ± 0.1	6.9 ± 0.7	11.1 ± 1.0	11.6 ± 1.7
La/Yb	-	11.5 ± 0.9	11.7 ± 0.6	11.5 ± 0.9	8.0 ± 1.1	8.7 ± 1.6	7.6 ± 0.6	21.2 ± 3.9	18.6 ± 2.9	-

Island	Stromboli			
Eruption	Secche di Lazzaro		18 NE	Upper Vancori
Sample Loc.	17 (N)			19
Sampled	Scoria	pumice	pumice	pumice
TAS	Tra-And* (U2)	Trachyte* (U5)	Trachyte†	Trachyte†
Nb/Zr	0.14 ± 0.01	0.14 ± 0.01	0.14 ± 0.01	0.13 ± 0.1
Nb/Th	1.25 ± 0.09	1.25 ± 0.09	1.28 ± 0.13	1.22 ± 0.13
Ta/Th	0.06 ± 0.005	0.06 ± 0.005	0.07 ± 0.01	0.06 ± 0.02
Zr/Th	8.9 ± 0.3	9.0 ± 0.5	9.1 ± 0.9	9.7 ± 0.5
La/Yb	24.9 ± 2.5	23.3 ± 3.4	22.6 ± 2.6	18.8 ± 2.5

Fig. 1

Fig. 2

(i) Palizzi B / Palizzi A

(j) Commenda Ash

(k) Upper Pollara

(l) Upper Pollara

(m) Monte Guardia / *Brown Tuff* / Lower Pollara 'Key bed' / *Brown Tuff*

(n) Lower Pollara / *Brown Tuff*

(o) U2 / U1 / Upper Vancori

(p) Present-day Stromboli / U5 / U4 / U3 / U2 / U1 / Secche di Lazzaro
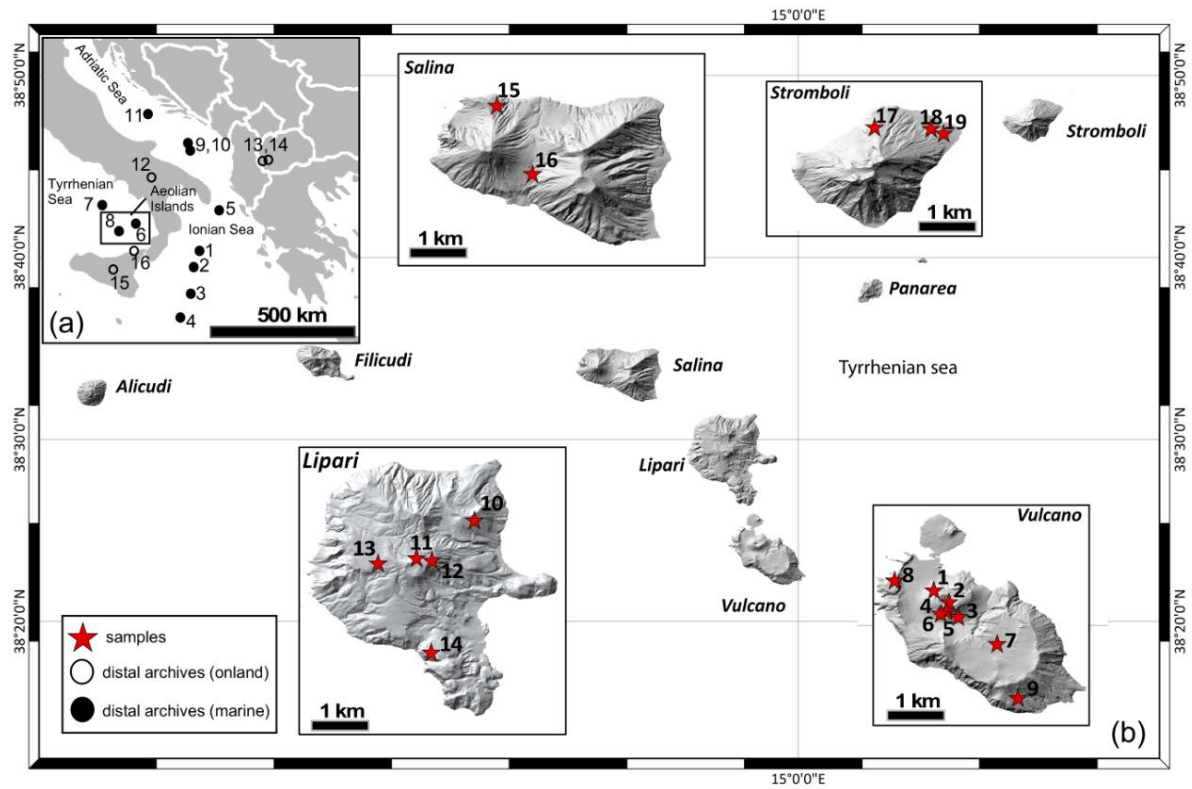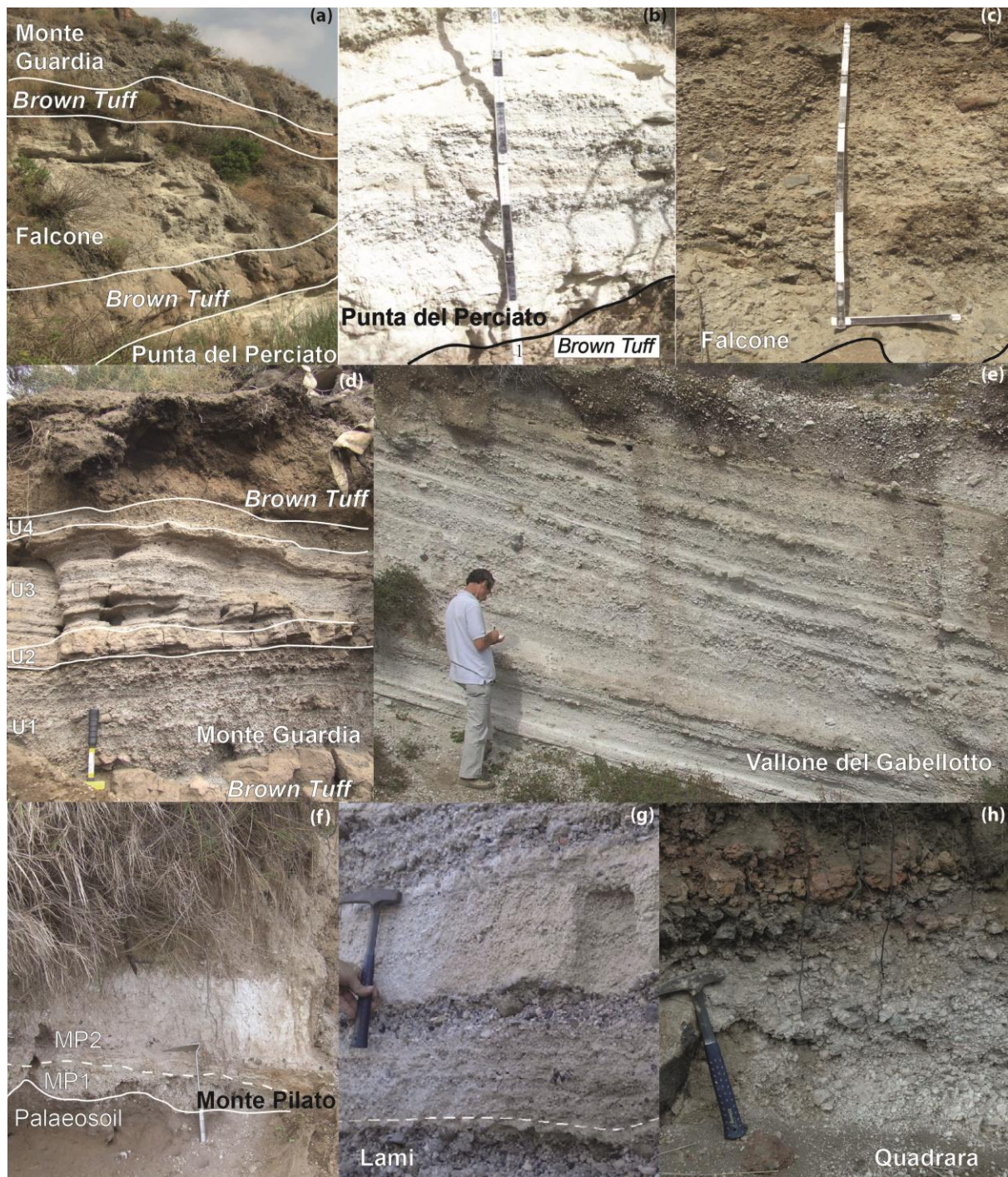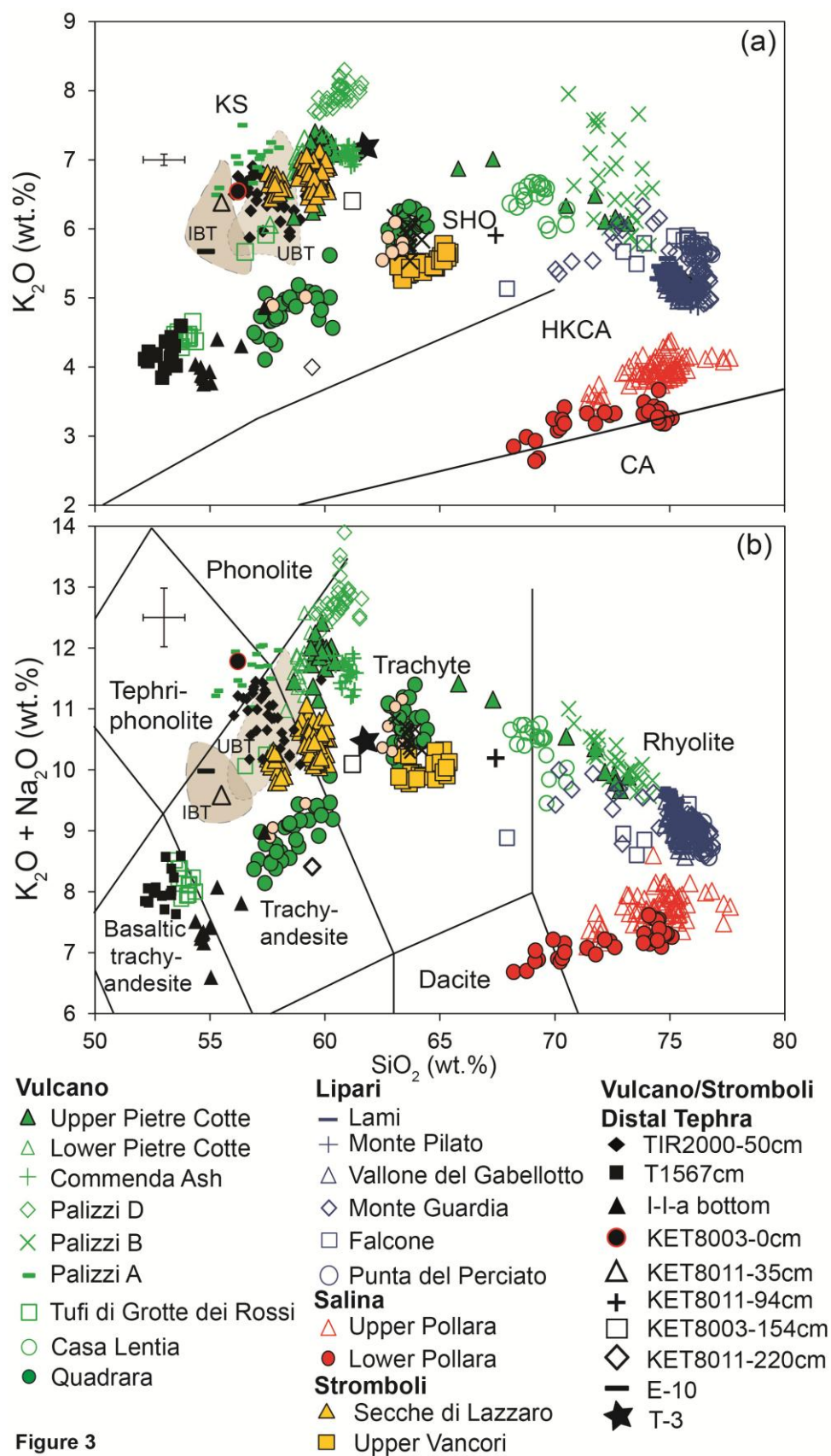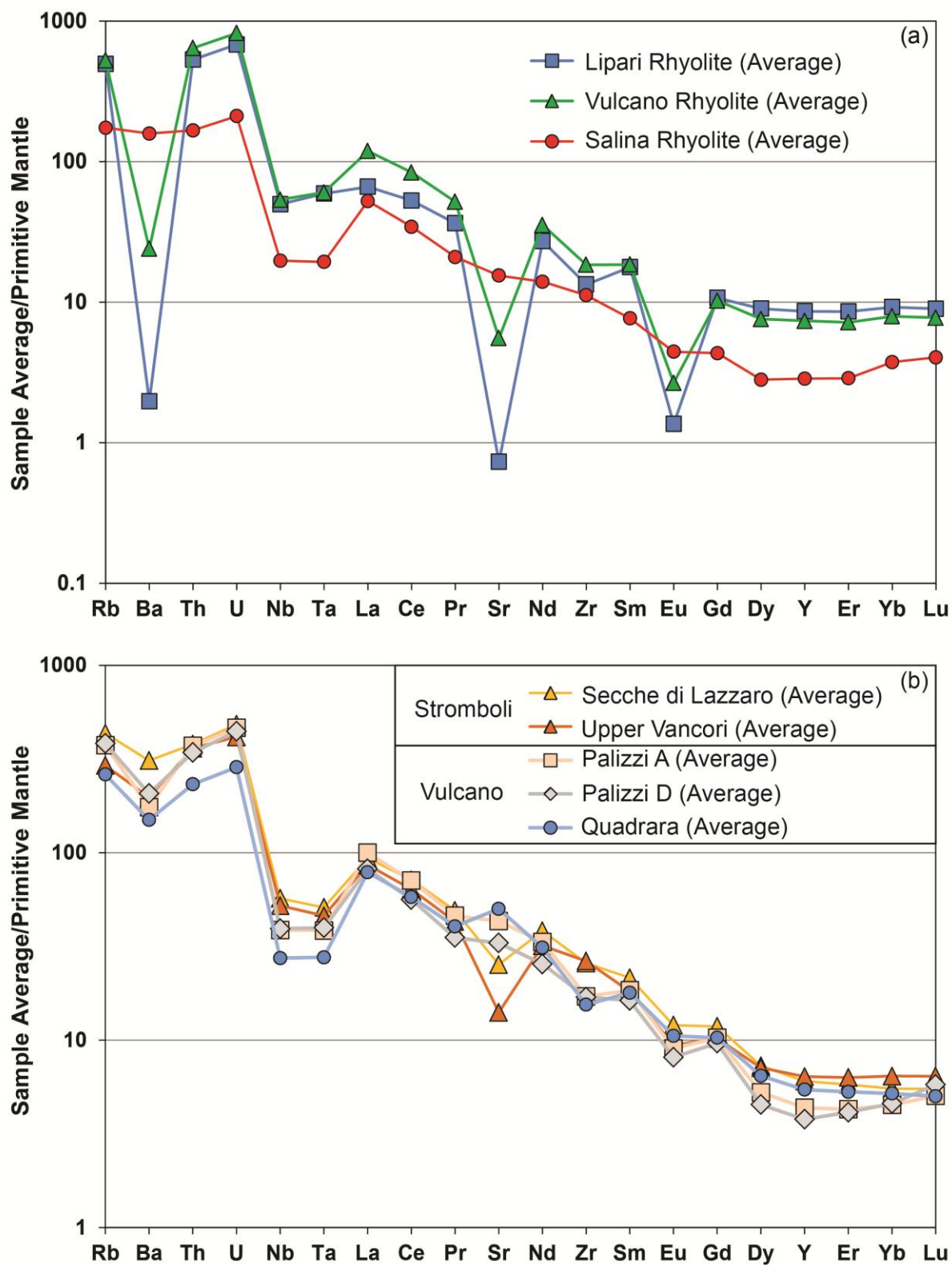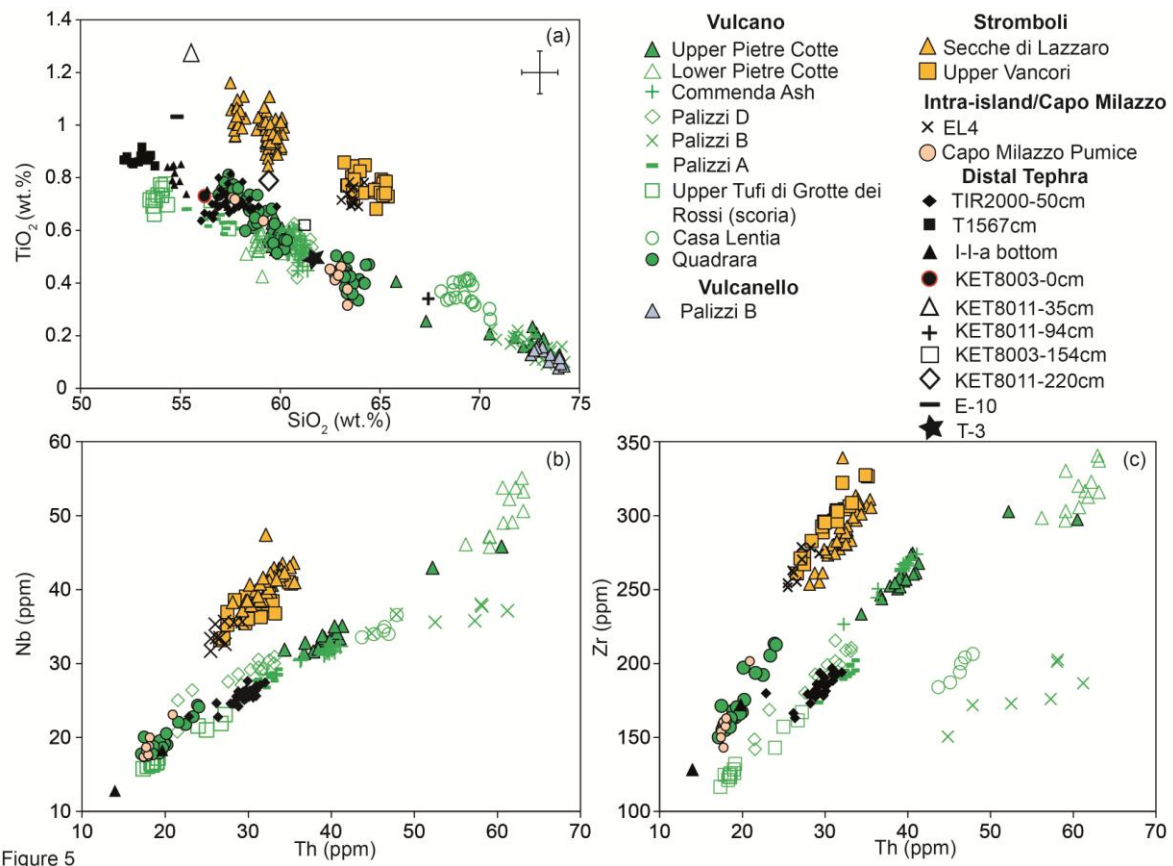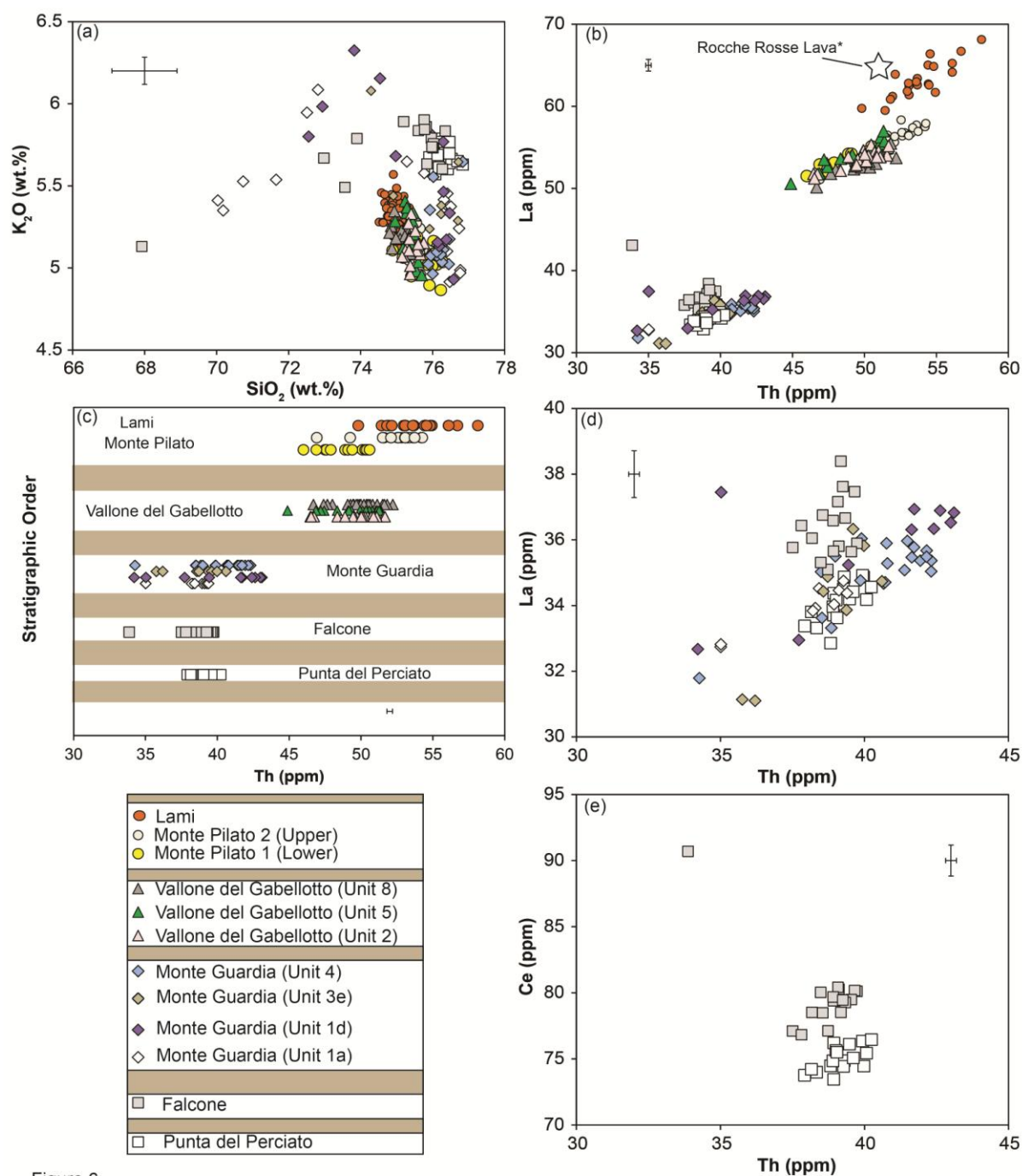
Fig. 3
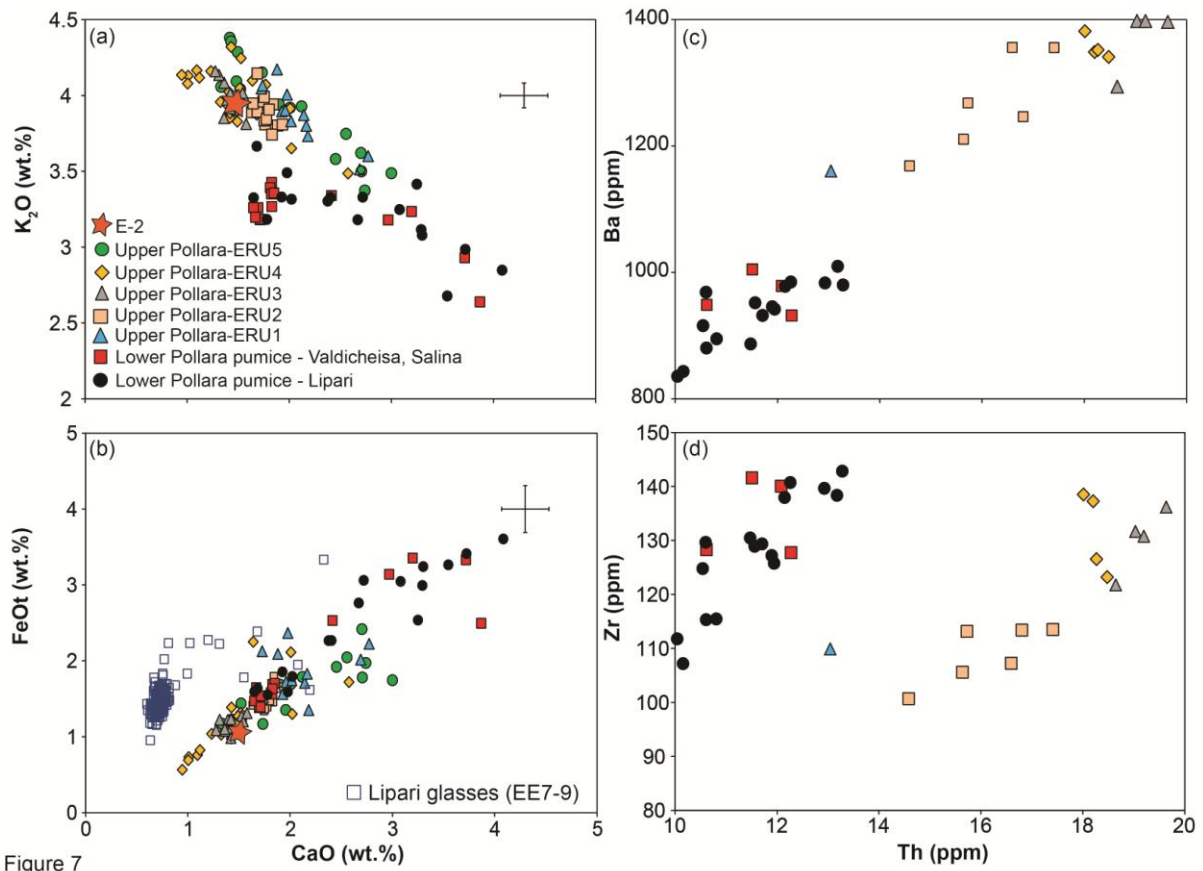

Figure 3

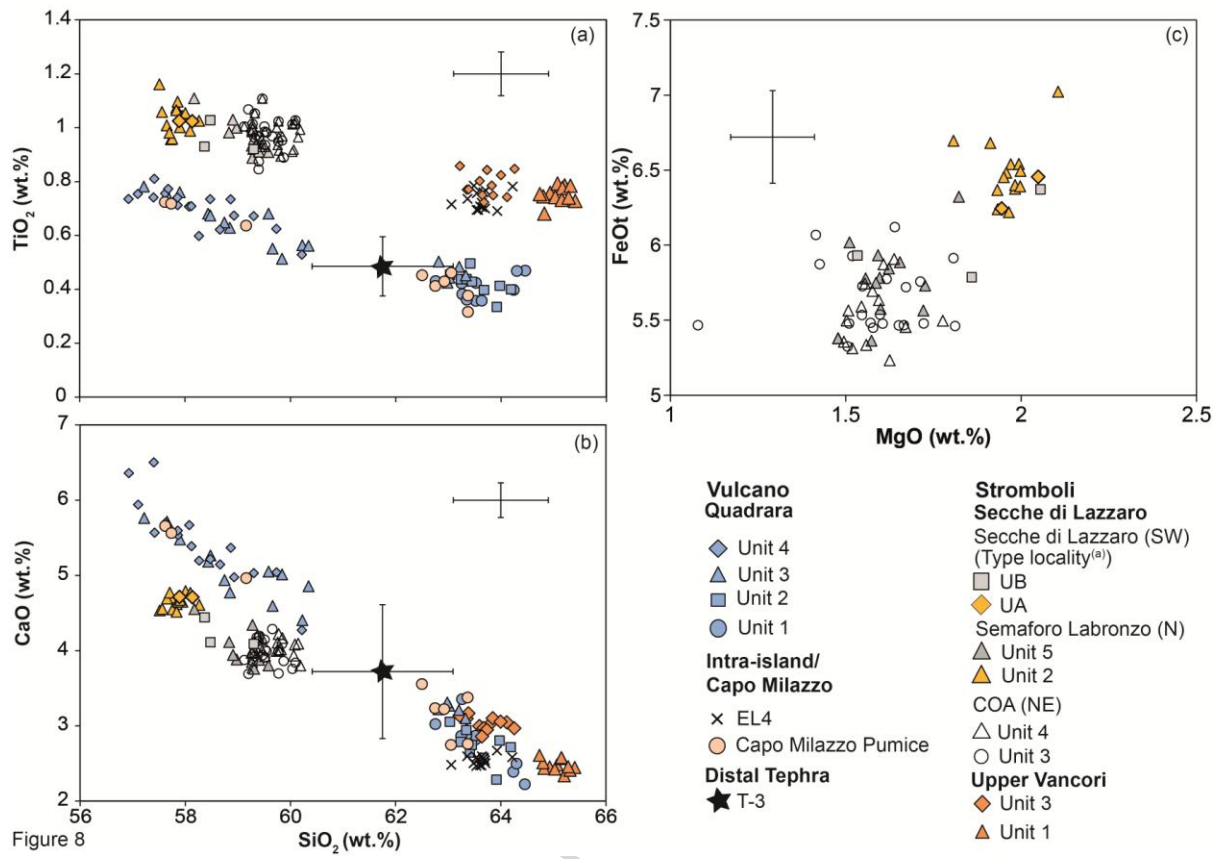Fig. 4

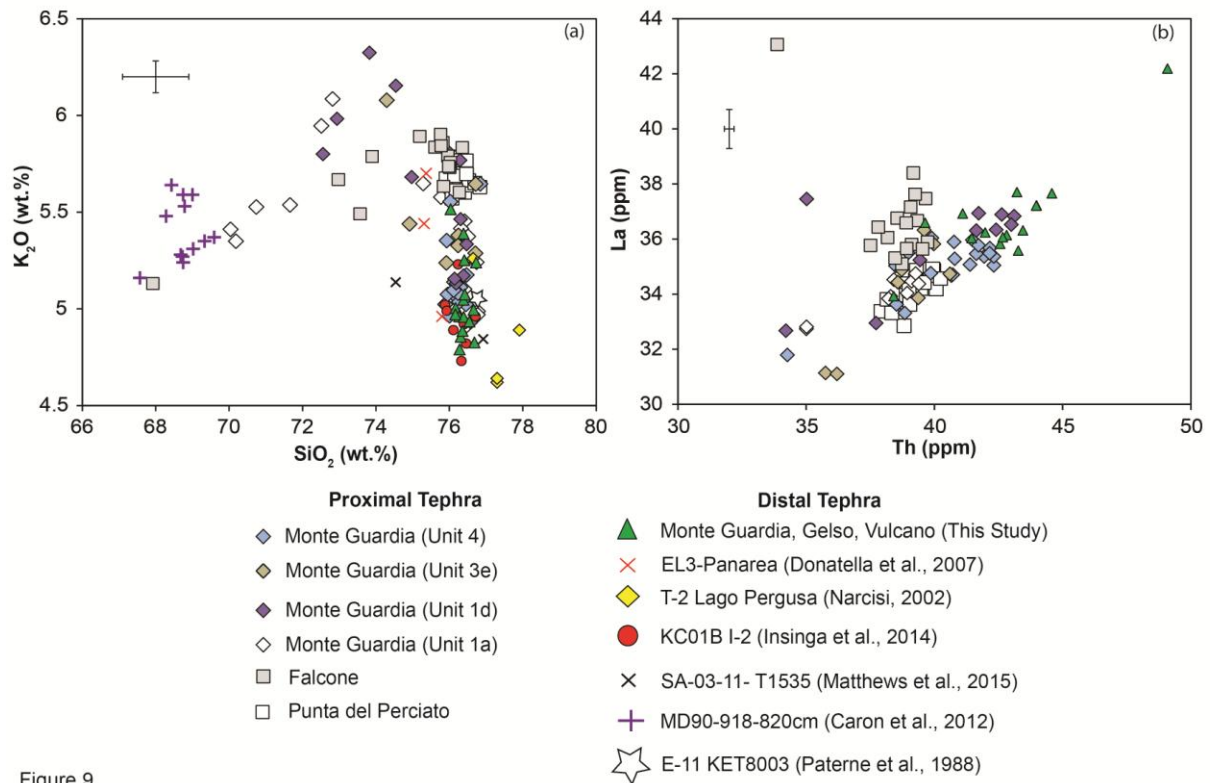Figure 4

Fig. 5

Figure 5

Fig. 6

Figure 6

Fig. 7

Figure 7

Fig. 8

Figure 8

Fig. 9

Figure 9

Proximal Tephra
- ◆ Monte Guardia (Unit 4)
- ◆ Monte Guardia (Unit 3e)
- ◆ Monte Guardia (Unit 1d)
- ◇ Monte Guardia (Unit 1a)
- ☐ Falcone
- ☐ Punta del Perciato

Distal Tephra
- ▲ Monte Guardia, Gelso, Vulcano (This Study)
- ✕ EL3-Panarea (Donatella et al., 2007)
- ◆ T-2 Lago Pergusa (Narcisi, 2002)
- ● KC01B I-2 (Insinga et al., 2014)
- ✕ SA-03-11- T1535 (Matthews et al., 2015)
- ✚ MD90-918-820cm (Caron et al., 2012)
- ☆ E-11 KET8003 (Paterne et al., 1988)
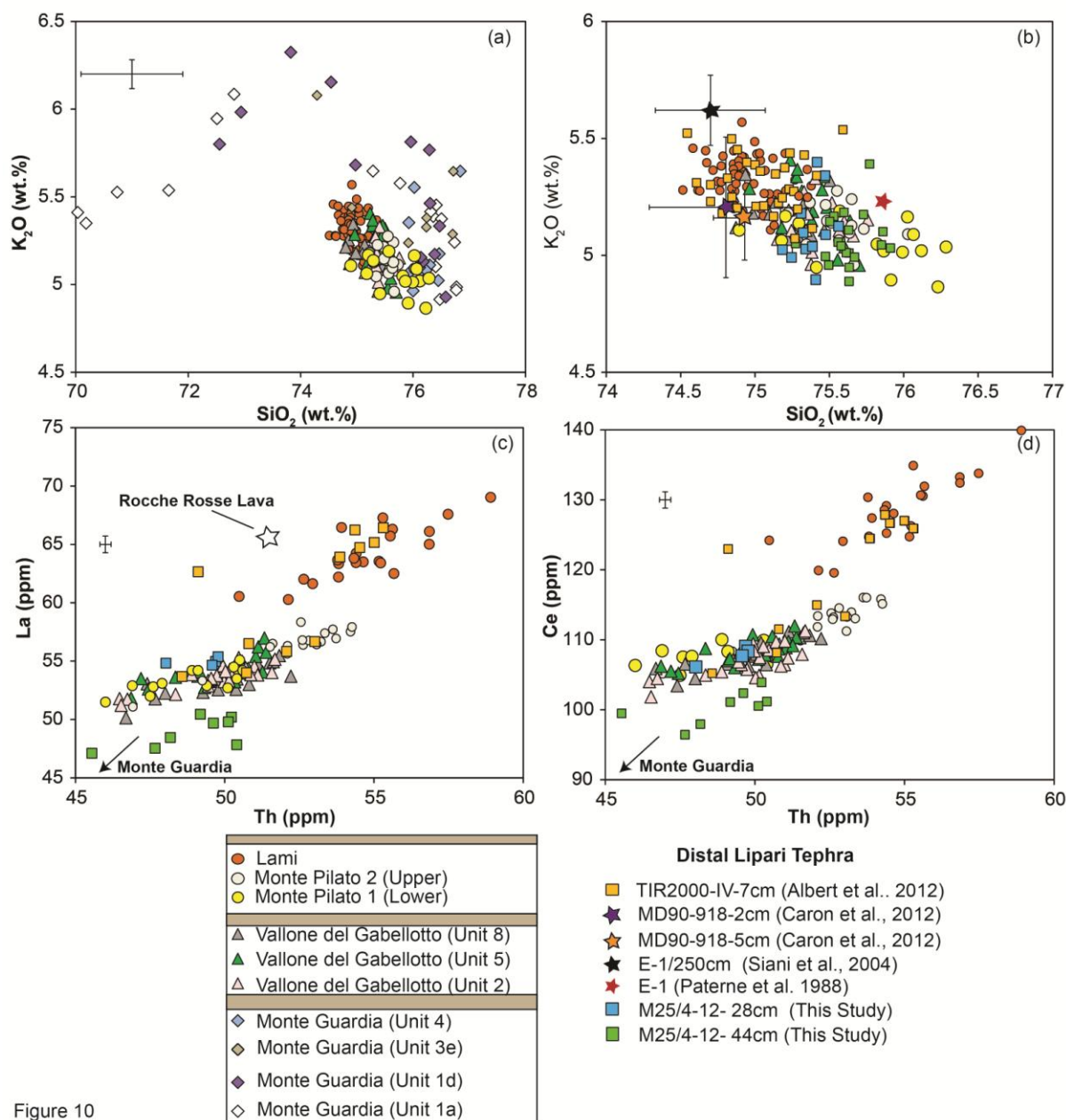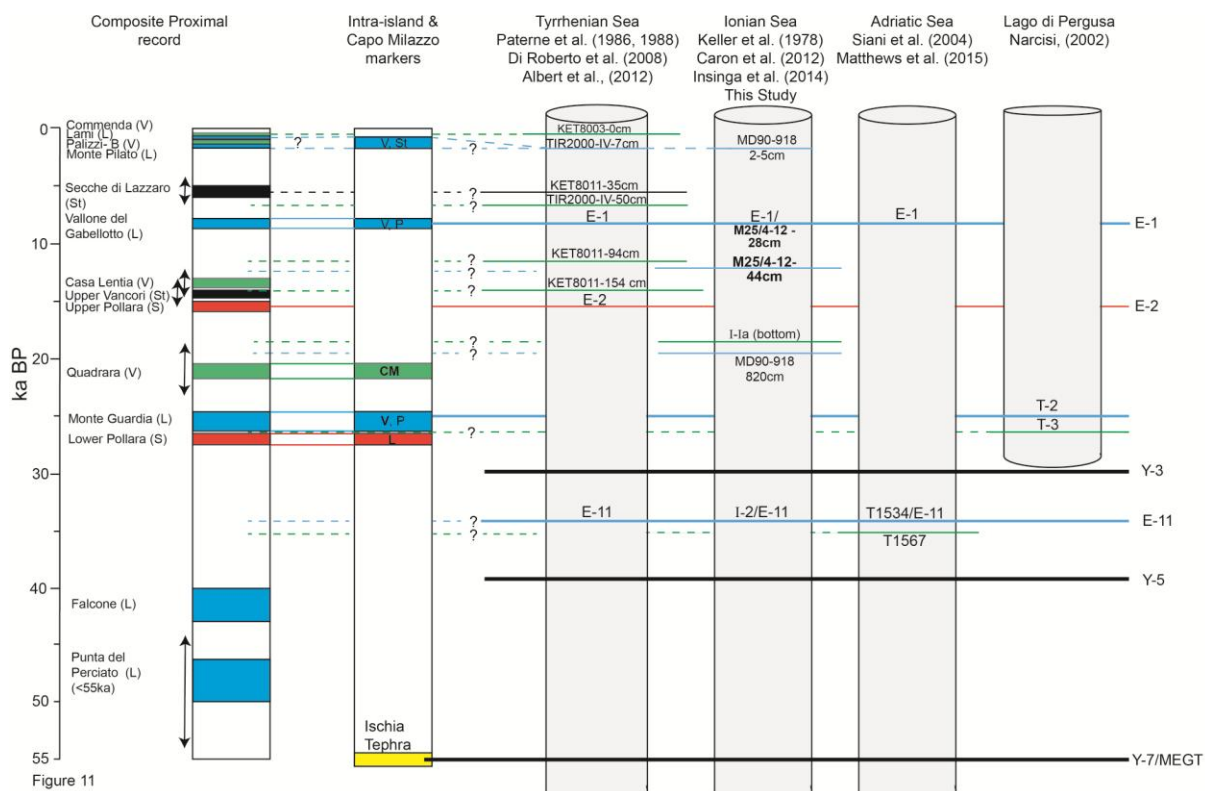
Fig. 10

Figure 10

Fig. 11

Figure 11

Highlights

- Glass characterisation (EMPA and LA-ICP-MS) of Aeolian Island tephra units
- Geochemical database
- Proximal-distal tephra correlations
- Proximal-distal composite event stratigraphy